EUROPEAN ORGANIZATION FOR NUCLEAR RESEARCH (CERN)

CERN-EP-2019-237
2020/03/16

CMS-EXO-19-002

Search for physics beyond the standard model in multilepton final states in proton-proton collisions at $\sqrt{s} = 13\,\text{TeV}$

The CMS Collaboration*

Abstract

A search for physics beyond the standard model in events with at least three charged leptons (electrons or muons) is presented. The data sample corresponds to an integrated luminosity of $137\,\text{fb}^{-1}$ of proton-proton collisions at $\sqrt{s} = 13\,\text{TeV}$, collected with the CMS detector at the LHC in 2016–2018. The two targeted signal processes are pair production of type-III seesaw heavy fermions and production of a light scalar or pseudoscalar boson in association with a pair of top quarks. The heavy fermions may be manifested as an excess of events with large values of leptonic transverse momenta or missing transverse momentum. The light scalars or pseudoscalars may create a localized excess in the dilepton mass spectra. The results exclude heavy fermions of the type-III seesaw model for masses below 880 GeV at 95% confidence level in the scenario of equal branching fractions to each lepton flavor. This is the most restrictive limit on the flavor-democratic scenario of the type-III seesaw model to date. Assuming a Yukawa coupling of unit strength to top quarks, branching fractions of new scalar (pseudoscalar) bosons to dielectrons or dimuons above 0.004 (0.03) and 0.04 (0.03) are excluded at 95% confidence level for masses in the range 15–75 and 108–340 GeV, respectively. These are the first limits in these channels on an extension of the standard model with scalar or pseudoscalar particles.

"Published in the Journal of High Energy Physics as `doi:10.1007/JHEP03(2020)051`*."*

*See Appendix A for the list of collaboration members

1 Introduction

A search for new phenomena in final states with at least three charged leptons (electrons or muons) is presented, using $137\,\text{fb}^{-1}$ of proton-proton (pp) collision data at $\sqrt{s} = 13\,\text{TeV}$ collected by the CMS experiment at the CERN LHC from 2016 to 2018. The results are interpreted in the context of two beyond the standard model (SM) theories, namely the type-III seesaw and light scalar or pseudoscalar sector extensions to the SM. The event selection and signal region definitions are chosen in a way that allows other models to be tested. Phenomenologically, these models show complementary signatures of resonant and nonresonant multilepton final states, as described below.

The seesaw mechanism introduces new heavy particles coupled to leptons and to the Higgs boson, in order to explain the light masses of the neutrinos [1–9]. Within the type-III seesaw model, the neutrino is assumed to be a Majorana particle whose mass arises via the mediation of new massive fermions. These massive fermions are an SU(2) triplet of heavy Dirac charged leptons ($\Sigma^{\pm}$) and a heavy Majorana neutral lepton (Σ^{0}). In pp collisions, these massive fermions may be pair-produced through electroweak interactions in both charged-charged and charged-neutral pairs. Multilepton final states arise from the decays of each of the $\Sigma^{+}\Sigma^{-}$, $\Sigma^{+}\Sigma^{0}$, and $\Sigma^{-}\Sigma^{0}$ pairs to the nine different pairs of W, Z, and Higgs bosons with SM leptons and the subsequent leptonic decays of the SM bosons. A complete decay chain example would be $\Sigma^{\pm}\Sigma^{0} \to (W^{\pm}\nu)(W^{\pm}\ell^{\mp}) \to (\ell^{\pm}\nu\nu)(\ell^{\pm}\nu\ell^{\mp})$, where ℓ and ν are the three flavors of charged and neutral SM leptons, respectively. All 27 distinct signal production and decay combinations of the seesaw signal are simulated [10]. The $\Sigma^{\pm,0}$ are degenerate in mass, their decays are prompt, and the Σ decay branching fractions are identical across all lepton flavors (flavor-democratic scenario). This is achieved by taking the mixing angles to be $V_{\text{e}} = V_{\mu} = V_{\tau} = 10^{-4}$, values that are compatible with the existing constraints [10–14].

New light scalars or pseudoscalars are a ubiquitous feature of many theories of physics beyond the SM, including, but not limited to, extended Higgs sectors, supersymmetric theories, and dark sector extensions [15–18]. We consider a generalization of a simple model [19, 20], where a new light CP-even scalar or CP-odd pseudoscalar boson (ϕ) is produced in pp collisions via a Yukawa coupling of the ϕ to top quarks, g_{t}, either in three-body associated production with top quark pairs, or in top quark pair production with three-body top quark decays, $\text{t} \to \text{bW}\phi$. The signal is collectively labeled as $\text{t}\bar{\text{t}}\phi$. In this paper, we search for decays of the ϕ boson via a Yukawa coupling to the charged leptons, g_{ℓ}, into dielectron or dimuon pairs within multilepton events. The decays of the ϕ boson into tau-tau lepton pairs are not considered. It is assumed that $g_{\ell} \ll g_{\text{t}}$ and that all other couplings of the ϕ boson are negligible. Furthermore, the ϕ boson decays are taken to be prompt, and the ϕ branching fractions into different flavors of charged lepton pairs, $\mathcal{B}(\phi \to \ell\ell)$, as well as g_{t}, are left as free parameters.

Figure 1 illustrates example diagrams for the production and decay of heavy fermions in the type-III seesaw model (left) and a light scalar or pseudoscalar boson in the $\text{t}\bar{\text{t}}\phi$ model (right).

Prior searches for the manifestation of the type-III seesaw model have been conducted by the ATLAS and CMS Collaborations using data recorded at $\sqrt{s} = 7$, 8, and 13 TeV [21–24]. The most stringent constraints in the flavor-democratic scenario are from a CMS search using 13 TeV data collected in 2016, which excluded Σ masses below 850 GeV [24]. The present study of the $\text{t}\bar{\text{t}}\phi$ model is the first direct search for a light scalar or pseudoscalar boson in leptonic decays produced in association with a top quark pair.

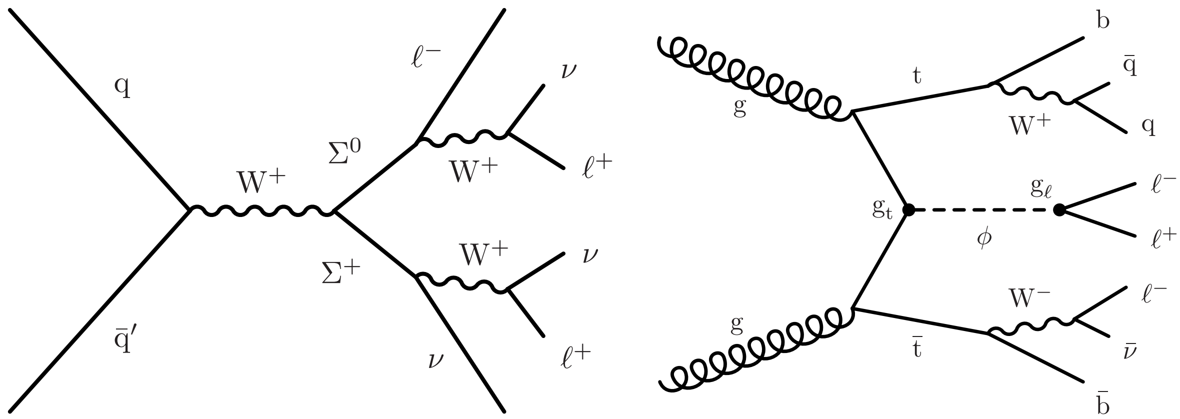

Figure 1: Leading order Feynman diagrams for the type-III seesaw (left) and $t\bar{t}\phi$ (right) signal models, depicting example production and decay modes in pp collisions.

2 The CMS detector

The central feature of the CMS apparatus is a superconducting solenoid of 6 m internal diameter, providing a magnetic field of 3.8 T. Within the solenoid volume are a silicon pixel and strip tracker, a lead tungstate crystal electromagnetic calorimeter (ECAL), and a brass and scintillator hadron calorimeter, each composed of a barrel and two endcap sections. Forward calorimeters extend the pseudorapidity (η) coverage provided by the barrel and endcap detectors. Muons are detected in gas-ionization chambers embedded in the steel flux-return yoke outside the solenoid. A more detailed description of the CMS detector, together with a definition of the coordinate system used and the relevant kinematic variables, can be found in Ref. [25]. The CMS detector uses a two-tiered trigger system [26]. The first level, composed of custom hardware processors, uses information from the calorimeters and muon detectors to select the most relevant pp collision events at rates up to 100 kHz. These are further processed by a second level consisting of a farm of processors, known as the high level trigger, that combines information from all CMS subdetectors to yield a final event rate of less than 1 kHz for data storage.

3 Data samples and event simulation

The data samples analyzed in this search correspond to a total integrated luminosity of 137 fb^{-1} (35.9, 41.5, and 59.7 fb^{-1} in years 2016, 2017 and 2018, respectively), recorded in pp collisions at $\sqrt{s} = 13$ TeV. A combination of isolated single-electron and single-muon triggers was used with corresponding transverse momentum (p_T) thresholds of 24 and 27 GeV in 2016, 27 and 32 GeV in 2017, and 24 and 32 GeV in 2018. Event samples from Monte Carlo (MC) simulations are used to estimate the rates of signal and relevant SM background processes. The WZ, $Z\gamma$, $t\bar{t}Z$, $t\bar{t}W$, and triboson backgrounds are generated using MADGRAPH5_aMC@NLO (2.2.2 in 2016, 2.4.2 in 2017 and 2018 data analyses) [27] at next-to-leading order (NLO) precision. The top quark mass used in all simulations is 172.5 GeV. The ZZ background contribution from quark-antiquark annihilation is generated using POWHEG 2.0 [28–30] at NLO, whereas the contribution from gluon-gluon fusion is generated at leading order (LO) using MCFM 7.0.1 [31]. Backgrounds from Higgs boson production for a Higgs boson mass of 125 GeV are generated at NLO using POWHEG and JHUGEN 7.0.11 [32–35]. Simulated event samples for Drell–Yan (DY) and $t\bar{t}$ processes, generated at NLO with MADGRAPH5_aMC@NLO and POWHEG, respectively, are used for systematic uncertainty studies.

All signal samples are simulated using MADGRAPH5_aMC@NLO 2.6.1 at LO precision. The production cross section for the type-III seesaw signal model $\sigma(\Sigma\Sigma)$ is calculated at NLO plus next-to-leading logarithmic precision, assuming that the heavy leptons are SU(2) triplet fermions [36, 37], while the $t\bar{t}\phi$ production cross section $\sigma(t\bar{t}\phi)$ comes directly from the MADGRAPH5_aMC@NLO 2.6.1 generator at LO precision.

All background and signal samples in 2016 are generated with the NNPDF3.0 NLO or LO parton distribution functions (PDFs), with the order matching that in the matrix element calculations. In 2017 and 2018, the NNPDF3.1 next-to-next-to-leading order PDFs [38, 39] are used. Parton showering, fragmentation, and hadronization for all samples are performed using PYTHIA 8.230 [40] with the underlying event tune CUETP8M1 [41] for the 2016 analysis, and CP5 [42] for the 2017 and 2018 analyses. Double counted partons generated with PYTHIA and MADGRAPH5_aMC@NLO are removed using the FxFx [43] matching schemes. The response of the CMS detector is simulated using dedicated software based on the GEANT4 toolkit [44], and the presence of multiple pp interactions in the same or adjacent bunch crossing (pileup) is incorporated by simulating additional interactions, that are both in-time and out-of-time with the hard collision according to the pileup in the data samples.

4 Event reconstruction

A particle-flow (PF) algorithm [45] aims to reconstruct and identify each individual particle in an event, with an optimized combination of information from the various elements of the CMS detector. In each event, the candidate vertex with the largest value of summed physics-object p_T^2 is taken to be the primary pp interaction vertex (PV). Here the physics objects are the jets, clustered using the jet finding algorithm [46, 47] with the tracks assigned to candidate vertices as inputs, and the associated missing transverse momentum, taken as the negative vector sum of the p_T of those jets. The energy of photons is obtained from the ECAL measurement. The energy of electrons is determined from a combination of the electron momentum at the PV as determined by the tracker, the energy of the corresponding ECAL cluster, and the energy sum of all bremsstrahlung photons spatially compatible with originating from the electron track. The energy of muons is obtained from the curvature of the corresponding track. The energy of charged hadrons is determined from a combination of their momentum measured in the tracker and the matching ECAL and HCAL energy deposits, corrected for zero-suppression effects and for the response function of the calorimeters to hadronic showers. Finally, the energy of neutral hadrons is obtained from the corresponding corrected ECAL and HCAL energies.

Jets used in this analysis are reconstructed using the anti-k_T algorithm [46] with a distance parameter of 0.4, as implemented in the FASTJET package [47]. Jets are required to have $p_T > 30$ GeV and, to be fully in the tracking system volume, $|\eta| < 2.1$. Jet momentum is determined as the vectorial sum of all particle momenta in the jet, and is found from simulation to be, on average, within 5–10% of the true momentum over the whole p_T spectrum and detector acceptance. The effect of the pileup on reconstructed jets is mitigated through a charged hadron subtraction technique, which removes the energy of charged hadrons not originating from the PV [45]. The impact of neutral pileup particles in jets is mitigated by an event-by-event jet-area-based correction of the jet four-momenta [48–50].

Jet energy corrections are derived from simulation studies so that the average measured response of jets becomes identical to that of particle level jets. In situ measurements of the momentum balance in dijet, photon+jet, leptonically decaying Z+jet, and multijet events are used to determine any residual differences between the jet energy scale in data and in simulation, and appropriate corrections are made to the jet p_T [50]. Additional quality criteria are applied to each jet to remove those potentially dominated by instrumental effects or reconstruction failures [51]. Finally, all selected jets are required to be outside a cone of $\Delta R \equiv \sqrt{(\Delta\eta)^2 + (\Delta\phi)^2} = 0.4$ around a selected electron or muon as defined below, where $\Delta\phi$ is the azimuthal distance.

A subset of these reconstructed jets originating from b hadrons is identified using the DeepCSV b tagging algorithm [52]. This algorithm has an efficiency of 60–75% to identify b quark jets, depending on jet p_{T} and η, and a misidentification rate of about 10% for c quark jets as well as 1% for light quark and gluon jets.

The missing transverse momentum vector $\vec{p}_{\mathrm{T}}^{\,\mathrm{miss}}$ is computed as the negative vector sum of the transverse momenta of all the PF candidates in an event, and its magnitude is denoted as $p_{\mathrm{T}}^{\mathrm{miss}}$ [53]. The $\vec{p}_{\mathrm{T}}^{\,\mathrm{miss}}$ is modified to account for corrections to the energy scale of the reconstructed jets in the event.

Electrons and muons are reconstructed by geometrically matching tracks reconstructed in the tracking system with energy clusters in the ECAL [54] and with the tracks in the muon detectors [55], respectively. Electrons are required to be within the tracking system acceptance, $|\eta| < 2.5$, and muons are required to be within the muon system acceptance, $|\eta| < 2.4$. Both electrons and muons must have $p_{\mathrm{T}} > 10\,\mathrm{GeV}$. Furthermore, electrons must satisfy shower shape and track quality requirements to suppress those originating from photon conversions in detector material as well as hadronic activity misidentified as electrons. Similarly, muons must satisfy track fit and matching quality requirements to suppress muon misidentification due to hadron shower remnants that reach the muon system.

Prompt isolated leptons produced by SM boson decays (either directly, or via an intermediate tau lepton) are indistinguishable from those produced in signal events. Thus, SM processes that can produce three or more isolated leptons, such as WZ, ZZ, $\mathrm{t\bar{t}Z}$, $\mathrm{t\bar{t}W}$, triboson, and Higgs boson production, constitute the irreducible backgrounds. Reducible backgrounds arise from SM processes, such as Z+jets or $\mathrm{t\bar{t}}$+jets production, accompanied by additional leptons originating from heavy quark decays or from misidentification of jets. Such leptons arising not from boson decays, but from leptons inside or near jets, hadrons that reach the muon detectors, or hadronic showers with large electromagnetic energy fractions, are referred to as misidentified leptons.

The reducible backgrounds are significantly suppressed by applying a set of lepton isolation and displacement requirements in addition to the quality criteria in the lepton identification [54, 55]. The relative isolation is defined as the scalar p_{T} sum, normalized to the lepton p_{T}, of photon and hadron PF objects within a cone of ΔR around the lepton. This relative isolation is required to be in the range of 5–15% for $\Delta R = 0.3$ for electrons, scaling inversely with the electron p_{T}, and to be less than 15% for $\Delta R = 0.4$ for muons. The isolation quantities are corrected for contributions from particles originating from pileup vertices. In addition to the isolation requirement, electrons must satisfy $|d_z| < 0.1\,\mathrm{cm}$ and $|d_{xy}| < 0.05\,\mathrm{cm}$ in the ECAL barrel ($|\eta| < 1.479$), and $|d_z| < 0.2\,\mathrm{cm}$ and $|d_{xy}| < 0.1\,\mathrm{cm}$ in the ECAL endcap ($|\eta| > 1.479$), where d_z and d_{xy} are the longitudinal and transverse impact parameters of electrons with respect to the primary vertex, respectively. Similarly, muons must satisfy $|d_z| < 0.1\,\mathrm{cm}$ and $|d_{xy}| < 0.05\,\mathrm{cm}$. All selected electrons within a cone of $\Delta R < 0.05$ of a selected muon are discarded, since these are possibly due to bremsstrahlung from the muons.

In trilepton events, where misidentified-background contributions are dominant, additional 3-dimensional impact parameter significance and b tag veto requirements are imposed on the leptons, removing those with significant displacement with respect to the PV or whose matching jet is b tagged. A PF jet with $p_{\mathrm{T}} > 10\,\mathrm{GeV}$ and $|\eta| < 2.5$ is considered to be matched if it is located within a cone of $\Delta R < 0.4$ around the lepton without any further quality criteria on the jet. These electron and muon reconstruction and selection requirements result in typical efficiencies of 40–90 and 75–95%, respectively, depending on the lepton p_{T} and η [54, 55].

5 Event selection

In both data and simulated event samples, events satisfying the trigger criteria are required to pass additional offline selections. Each event is required to have at least one electron with $p_{\mathrm{T}} > 35\,\mathrm{GeV}$ (30 GeV in 2016) or at least one muon with $p_{\mathrm{T}} > 26\,\mathrm{GeV}$ (29 GeV in 2017) to be consistent with the trigger thresholds, depending on the trigger used to collect the event. Throughout this analysis, we consider events with exactly 3 leptons (3L) in one category and four or more leptons (4L) in another category. In the 4L event category, only the 4 leading-p_{T} leptons are considered. All events containing a lepton pair with $\Delta R < 0.4$ or a same-flavor lepton pair with dilepton invariant mass below 12 GeV are removed to reduce background contributions from low-mass resonances as well as final-state radiation. The 3L events containing an opposite-sign same-flavor (OSSF) lepton pair with the dilepton invariant mass below 76 GeV, when the trilepton invariant mass is within a Z boson mass window ($91 \pm 15\,\mathrm{GeV}$), are also rejected. This suppresses events from the $\mathrm{Z} \to \ell\ell^{*} \to \ell\ell\gamma$ background process, where the photon converts into two additional leptons, one of which is lost. The event selection criteria for both the type-III seesaw and $\mathrm{t\bar{t}}\phi$ signal models are orthogonal to those used in the estimation of SM backgrounds.

In the context of the type-III seesaw extension of the SM, pair production of heavy fermions gives rise to events with multiple energetic charged leptons or neutrinos in the final state. Given the relatively high momenta of bosons and leptons originating from the decays of these heavy particles, kinematic quantities, such as the scalar p_{T} sum of all leptons, are instrumental in suppressing SM contributions. This is especially valid for decay modes such as $\Sigma^{\pm} \to \ell^{\pm}\mathrm{Z} \to \ell^{\pm}\ell^{\pm}\ell^{\mp}$, where all of the daughter particles of the heavy fermion can be reconstructed in the detector. However, $p_{\mathrm{T}}^{\mathrm{miss}}$ can be used as a complementary kinematic quantity in other decay modes, such as $\Sigma^{0} \to \nu\mathrm{H} \to \nu\mathrm{W}^{\pm}\mathrm{W}^{\mp}$ or $\Sigma^{\pm} \to \nu\mathrm{W}^{\pm} \to \nu\ell^{\pm}\nu$, where neutrinos can carry a significant fraction of the outgoing momentum. We define L_{T} as the scalar p_{T} sum of all charged leptons, and the quantity $L_{\mathrm{T}}+p_{\mathrm{T}}^{\mathrm{miss}}$ is chosen as the primary kinematic discriminant to select this variety of decay modes.

We classify the selected multilepton events into statistically independent search channels using the multiplicity of leptons, N_{leptons}, as well as the multiplicity and mass of distinct OSSF pairs, N_{OSSF} and M_{OSSF}, respectively. In cases of ambiguity, M_{OSSF} is calculated using the OSSF pair with the mass closest to that of the Z boson, considering both electrons and muons. The 3L events with an OSSF lepton pair are labeled as OSSF1, whereas those without are labeled as OSSF0. The OSSF1 events are further classified as on-Z, below-Z, and above-Z, based on the M_{OSSF} relative to the $\pm 15\,\mathrm{GeV}$ window around the Z boson mass, where the latter two categories are also collectively labeled as off-Z. Similarly, the 4L events are classified as those with zero, one, and two distinct OSSF lepton pairs, OSSF0, OSSF1, and OSSF2, respectively.

In the 3L on-Z search region, the sensitivity is increased by considering the transverse mass discriminant $M_{\mathrm{T}} = \sqrt{2p_{\mathrm{T}}^{\mathrm{miss}}p_{\mathrm{T}}^{\ell}[1-\cos(\Delta\phi_{\vec{p}_{\mathrm{T}}^{\mathrm{miss}},\vec{p}_{\mathrm{T}}^{\ell}})]}$ instead of $L_{\mathrm{T}}+p_{\mathrm{T}}^{\mathrm{miss}}$, where ℓ refers to the lepton that is not part of the on-Z pair. We reject 3L on-Z events with $p_{\mathrm{T}}^{\mathrm{miss}} < 100\,\mathrm{GeV}$, and 4L OSSF2 events with $p_{\mathrm{T}}^{\mathrm{miss}} < 100\,\mathrm{GeV}$ and two distinct OSSF lepton pairs on-Z, as these are used in the estimation of SM backgrounds.

This event selection and binning scheme yields a total of 40 statistically independent search bins for the type-III seesaw model, as summarized in Table 1.

Table 1: Multilepton signal region definitions for the type-III seesaw signal model. All events containing a same-flavor lepton pair with invariant mass below 12 GeV are removed in the 3L and 4L event categories. Furthermore, 3L events containing an OSSF lepton pair with mass below 76 GeV when the trilepton mass is within a Z boson mass window (91 $\pm$ 15 GeV) are also rejected. The last L_T+p_T^{miss} or M_T bin in each signal region contains the overflow events.

Label	$N_{leptons}$	N_{OSSF}	M_{OSSF} (GeV)	p_T^{miss} (GeV)	Variable and range (GeV)		Number of bins
3L below-Z	3	1	<76	—	L_T+p_T^{miss}	$[0, 1200]$	6
3L on-Z	3	1	76–106	>100	M_T	$[0, 700]$	7
3L above-Z	3	1	>106	—	L_T+p_T^{miss}	$[0, 1600]$	8
3L OSSF0	3	0	—	—	L_T+p_T^{miss}	$[0, 1200]$	6
4L OSSF0	≥4	0	—	—	L_T+p_T^{miss}	$[0, 600]$	2
4L OSSF1	≥4	1	—	—	L_T+p_T^{miss}	$[0, 1000]$	5
4L OSSF2	≥4	2	—	>100 if both pairs are on-Z	L_T+p_T^{miss}	$[0, 1200]$	6

In contrast, the $t\bar{t}\phi$ model yields events with a resonant OSSF lepton pair originating from the ϕ decays produced in association with a $t\bar{t}$ pair. We consider only 3L or 4L events with at least one OSSF lepton pair and exclude those with M_{OSSF} on-Z. This event selection requires semileptonic or dileptonic $t\bar{t}$ decays in the $t\bar{t}\phi$ signal. Unlike the type-III seesaw heavy fermions, relatively light scalar or pseudoscalar decays do not necessarily produce energetic charged leptons, but can yield striking resonant dilepton signatures in events with high hadronic activity and b tagged jets. Therefore, we seek events with resonances in the OSSF dilepton mass spectra in various S_T bins, where S_T is defined as the scalar p_T sum of all jets, all charged leptons (L_T) and p_T^{miss}.

We probe the $t\bar{t}\phi$ signal in light and heavy ϕ mass ranges, namely 15–75 and 108–340 GeV. Signal masses below 15 GeV and in the range of 75–108 GeV are not considered because of background from low-mass quarkonia and Z boson resonances, respectively. Masses above 340 GeV are not considered as the $\phi \to t\bar{t}$ decay channel becomes kinematically accessible here.

To account for the effects of radiation and resolution on the invariant mass reconstruction, we consider the 12–77 GeV (low) and 106–356 GeV (high) reconstructed dilepton mass ranges for the light and heavy signal mass scenarios, respectively, in both 3L and 4L channels. Because there can be an ambiguity caused by additional leptons originating from the $t\bar{t}$ system, the reconstruction of the correct ϕ mass is not always possible. Therefore, we define the M_{OSSF}^{20} and the M_{OSSF}^{300} variables as the OSSF lepton pair masses of a given lepton flavor closest to the targeted mass of 20 and 300 GeV, respectively. The M_{OSSF}^{20} variable is used for the low dilepton mass range, while the M_{OSSF}^{300} variable is used for the high dilepton mass range. Events with a value of M_{OSSF}^{20} (M_{OSSF}^{300}) outside the low (high) dilepton mass ranges are not considered. The analysis is insensitive to the choice of the targeted mass value, and this simplified scheme allows multiple $t\bar{t}\phi$ signal scenarios to be probed with a single mass spectrum.

The M_{OSSF}^{20} and M_{OSSF}^{300} masses are calculated separately for each lepton flavor scenario, yielding two nonorthogonal categories labeled as 3/4L(ee) and 3/4L($\mu\mu$). Hence, a given event can qualify for both the low and high dilepton mass regions, as well as for both lepton flavor channels. For example, a $\mu^{\pm}\mu^{\pm}\mu^{\mp}$ event could be present in both low and high dilepton mass regions in the 3L($\mu\mu$) category, and similarly, an $e^{\pm}e^{\mp}\mu^{\pm}\mu^{\mp}$ event could qualify for both the 4L(ee) and 4L($\mu\mu$) categories. However, for any one given $t\bar{t}\phi$ signal mass and flavor scenario, only one of the dilepton mass ranges of a single flavor category is considered.

Events that satisfy the low or high dilepton mass ranges are considered in orthogonal $N_b = 0$

Table 2: Multilepton signal region definitions for the $t\bar{t}\phi$ signal model. All events containing a same-flavor lepton pair with invariant mass below 12 GeV are removed in the 3L and 4L event categories. Furthermore, 3L events containing an OSSF lepton pair with mass below 76 GeV when the trilepton mass is within a Z boson mass window (91 ± 15 GeV) are also rejected.

Label	N_{leptons}	N_{OSSF}	M_{OSSF}	N_{b}	Variable and range (GeV)		Number of bins		
						S_{T} (GeV)	0–400	400–800	>800
3L(ee/$\mu\mu$) 0B	3	1	off-Z	0	M_{OSSF}^{20}	[12, 77]	13	13	5
					M_{OSSF}^{300}	[106, 356]	10	10	10
3L(ee/$\mu\mu$) 1B	3	1	off-Z	$\geq$1	M_{OSSF}^{20}	[12, 77]	13	13	5
					M_{OSSF}^{300}	[106, 356]	10	10	10
						S_{T} (GeV)	0–400	>400	
4L(ee/$\mu\mu$) 0B	$\geq$4	$\geq$1	off-Z	0	M_{OSSF}^{20}	[12, 77]	3	2	
					M_{OSSF}^{300}	[106, 356]	3	2	
						S_{T} inclusive			
4L(ee/$\mu\mu$) 1B	$\geq$4	$\geq$1	off-Z	$\geq$1	M_{OSSF}^{20}	[12, 77]	3		
					M_{OSSF}^{300}	[106, 356]	3		

(0B) and $N_{\text{b}} \geq 1$ (1B) selections, where N_{b} is the multiplicity of b tagged jets in an event. Events in the 3L signal channels are further split into 3 S_{T} bins (0–400 GeV, 400–800 GeV, and $\geq$800 GeV) for both N_{b} selections, those in the 4L signal channels are split into 2 S_{T} (0–400 GeV and $\geq$400 GeV) bins for the 0B selection, and only one inclusive bin in S_{T} is used for the 1B selection.

This event selection and binning scheme results in a total of 70 (68) statistically independent low (high) dilepton mass search bins in each of the 3/4L(ee) and 3/4L($\mu\mu$) channels for the $t\bar{t}\phi$ signal model, as summarized in Table 2. The signal mass hypotheses that are closer to the mass bin boundaries than to the bin centers are probed with a modified binning scheme, where the mass bin boundaries are shifted by half the value of the bin widths.

6 Background estimation and systematic uncertainties

The irreducible backgrounds are estimated using simulated event samples and are dominated by the WZ, ZZ, $t\bar{t}Z$, and $Z\gamma$ processes. The event yields of these processes are obtained from theoretical predictions, with normalization corrections derived in dedicated control regions as described below. These estimates for the WZ, ZZ and $Z\gamma$ processes are largely independent of each other. Since these backgrounds make significant contributions to the $t\bar{t}Z$-enriched control region, the normalization correction for this process is measured after the corresponding corrections have been obtained for the other backgrounds. The normalization correction factors and their associated uncertainties, which include both statistical and systematic contributions, take the contamination of events from other processes into account and are applied to the corresponding background estimates in the signal regions.

For the WZ and $t\bar{t}Z$ processes, we select events with exactly three leptons with an on-Z OSSF pair, and the minimum lepton p_{T} is required to be above 20 GeV to increase the purity of these selections in the targeted process. For the WZ-enriched selection, we require $50 < p_{\text{T}}^{\text{miss}} < 100$ GeV and zero b tagged jets, whereas for the $t\bar{t}Z$-enriched selection we require $p_{\text{T}}^{\text{miss}} < 100$ GeV, $S_{\text{T}} > 350$ GeV, and at least one b tagged jet. Similarly, for ZZ, we select events with exactly four leptons, $p_{\text{T}}^{\text{miss}} < 100$ GeV, and two distinct on-Z OSSF lepton pairs. In the WZ- and ZZ-enriched selections, the simulated event yields are normalized to match those in the data in

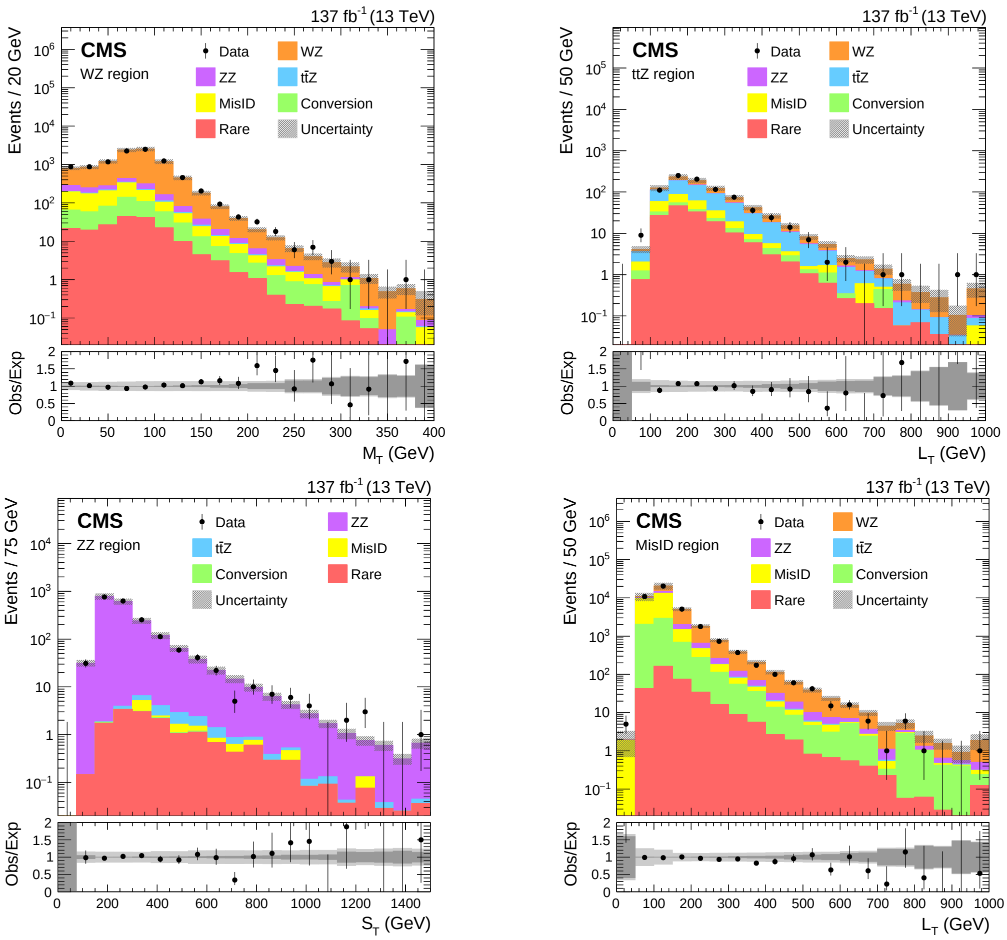

Figure 2: The M_T distribution in the WZ-enriched control region (upper left), the L_T distribution in the $t\bar{t}Z$-enriched control region (upper right), the S_T distribution in the ZZ-enriched control region (lower left), and the L_T distribution in the misidentified-lepton (Z+jets) enriched control region (lower right). The lower panels show the ratio of observed to expected events. The hatched gray bands in the upper panels and the light gray bands in the lower panels represent the total (systematic and statistical) uncertainty of the backgrounds in each bin, whereas the dark gray bands in the lower panels represent only the statistical uncertainty of the backgrounds. The rightmost bins contain the overflow events in each distribution.

the 0–3 and 0–2 jet multiplicity bins including overflows, respectively, yielding normalization factor uncertainties in the range of 5–25%, whereas an inclusive normalization is performed in the $t\bar{t}Z$-enriched selection, resulting in a 20% uncertainty. The various kinematic distributions in the WZ-, ZZ-, and $t\bar{t}Z$-enriched control regions, where the normalizations of these major irreducible backgrounds are performed, are illustrated in Fig. 2 (top-left, top-right, bottom-left).

Similarly, a $Z\gamma$-enriched selection is created in three-lepton events with an OSSF lepton pair with mass below 76 GeV and trilepton mass within the Z boson mass window, 91 ± 15 GeV. This selection is dominated by Z+jets events with internal and external photon conversions originating from final-state radiation, and the normalization yields a relative uncertainty of 20%. Conversion contributions from non-$Z\gamma$ processes play a subdominant role, and are estimated using simulated event samples.

Other irreducible backgrounds, such as $t\bar{t}W$, triboson, and Higgs boson processes, are estimated via simulation as well, using the cross sections obtained from the MC generation at NLO or higher accuracy, and are collectively referred to as 'rare' backgrounds. All rare and non-$Z\gamma$ conversion backgrounds, which are not normalized to data in dedicated control regions, are assigned a relative normalization uncertainty of 50%.

A small fraction of the irreducible backgrounds are due to misidentification of the charge of one or more prompt electrons. These backgrounds are also estimated using simulated event samples. Following a study of same-sign dielectron events, in which the dielectron invariant mass is within a Z boson mass window (91 ± 15 GeV), a relative uncertainty of 50% is assigned to such contributions. These constitute less than 35% of the irreducible WZ, ZZ, and $t\bar{t}Z$ background contributions in the 3L OSSF0, 4L OSSF1, and 4L OSSF0 signal regions, and are negligible in all other signal regions.

A category of systematic uncertainties in the simulated events is due to the corrections applied to background and signal simulation samples to account for differences with respect to data events. These corrections are used in lepton reconstruction, identification, isolation, and trigger efficiencies, b tagging efficiencies, pileup modeling, as well as electron and muon resolution, and electron, muon, jet, and unclustered energy scale measurements. The uncertainties due to such corrections typically correspond to a 1–10% variation of the simulation-based irreducible background and signal yields across all signal regions. Therefore, they form a sub-dominant category of systematic uncertainties in the simulation-based background estimation. Similarly, uncertainties due to choices of factorization and renormalization scales [56] and PDFs [39] are also evaluated for signal and dominant irreducible background processes, yielding $<$10% variation in signal regions. The uncertainties in the integrated luminosity are in the range of 2.3–2.5% in each year of data collection [57–59].

The reducible backgrounds are due to misidentified leptons (MisID) arising from events such as Z+jets and $t\bar{t}$+jets. These are estimated using a three-dimensional implementation of a matrix method [60], in which the rates at which prompt and misidentified leptons satisfying a loose lepton selection also pass a tight lepton selection are measured in dedicated signal-depleted selections of events in data. The misidentification rates are measured in Z+jets and $t\bar{t}$+jets enriched trilepton (on-Z, $p_T^{miss} < 50$ GeV) and same-sign dilepton (off-Z, $p_T^{miss} > 50$ GeV, and with at least 3 jets) selections, respectively, whereas an on-Z dilepton selection is used for the prompt rates. The rates are parametrized as a function of lepton kinematic distributions and the multiplicity of tracks in the event. A weighted average of these misidentification rates is used in the analysis, reflecting the approximate expected composition of the SM backgrounds in a given search region as obtained from simulated event samples. The final uncertainty in the estimated

Table 3: Sources of systematic uncertainties, affected background and signal processes, relative variations of the affected processes, and presence or otherwise of correlation between years in signal regions.

Uncertainty source	Signal/Background process	Variation (%)	Correlation
Integrated Luminosity	Signal/Rare/Non-Zγ conversion	2.3–2.5	No
Lepton reconstruction, identification, and isolation efficiency	Signal/Background*	4–5	No
Lepton displacement efficiency (only in 3L)	Signal/Background*	3–5	Yes
Trigger efficiency	Signal/Background*	$<$3	No
b tagging efficiency	Signal/Background*	$<$5	No
Pileup modeling	Signal/Background*	$<$3	Yes
Factorization/renormalization scales & PDF	Signal/Background*	$<$10	Yes
Jet energy scale	Signal/Background*	$<$5	Yes
Unclustered energy scale	Signal/Background*	$<$5	Yes
Muon energy scale and resolution	Signal/Background*	$<$5	Yes
Electron energy scale and resolution	Signal/Background*	$<$2	Yes
WZ normalization (0/1/2/$\geq$3 jets)	WZ	5–10	Yes
ZZ normalization (0/1/$\geq$2 jets)	ZZ	5–10	Yes
$\mathrm{t\bar{t}Z}$ normalization	$\mathrm{t\bar{t}Z}$	15–20	Yes
Conversion normalization	Conversion	20–50	Yes
Rare normalization	Rare	50	Yes
Lepton misidentification rates	Misidentified lepton	30–40	Yes
Electron charge misidentification	WZ/ZZ†	$<$20	No

*WZ, ZZ, $\mathrm{t\bar{t}Z}$, rare, and conversion background processes.
†Only in 3L OSSF0, 4L OSSF0, and 4L OSSF1 signal regions.

background from misidentified leptons is obtained by varying the rates within the uncertainties as well as the differences in rates in Z+jets and $\mathrm{t\bar{t}}$+jets events, and has a relative uncertainty of 30–40%. Figure 2 (lower right) illustrates the misidentified-lepton background estimate as a function of L_T in the trilepton selection used to measure the rates, where a misidentified lepton is produced in association with a Z boson.

A summary of the uncertainty sources in this analysis, including the typical resultant variations on relevant background and signal processes, as well as the correlation model across the three different data taking periods, is given in Table 3. The quoted variations on affected processes, except those in the integrated luminosity, and the inclusive normalizations of the $\mathrm{t\bar{t}Z}$, conversion and rare simulations, are calculated taking into account variations of the uncertainty sources as a function of object and event dependent parameters as appropriate, such as lepton momenta, or jet multiplicity. Thus, these uncertainties also include bin-to-bin correlations across the search regions. The overall uncertainties in the total expected backgrounds are largely dominated by those in the irreducible WZ, ZZ, and $\mathrm{t\bar{t}Z}$ processes, as well as the misidentified-lepton contributions, whereas the relatively large uncertainties in rare and conversion contributions and those due to electron charge misidentification are subdominant and have a negligible effect on the results across different signal regions.

7 Results

The distributions of expected SM backgrounds and observed event yields in the signal regions as defined in Tables 1 and 2 are given in Figs. 3–4 and 5–10 for the type-III seesaw model and the $\mathrm{t\bar{t}}\phi$ model, respectively. The figures also show the predicted yields for type-III seesaw models with Σ masses of 300 and 700 GeV in the flavor-democratic scenario as well as for $\mathrm{t\bar{t}}\phi$ models with a pseudoscalar (scalar) ϕ mass of 20 and 125 (70 and 300) GeV assuming $g_\mathrm{t}^2\mathcal{B}(\phi \to$

ee/$\mu\mu$) = 0.05.

We perform a goodness-of-fit test based on the saturated model method [61] to quantify the local deviations between the background-only hypothesis and the observed data, without considering the look-elsewhere effect [62]. The most significant local deviation from the SM expectation in the signal regions is found in the 3L($\mu\mu$) 1B $S_T < 400\,\text{GeV}$ high mass $t\bar{t}\phi$ channel (Fig. 9) by selecting the bins with $M_{\text{OSSF}}^{300} > 206\,\text{GeV}$, resulting in a data excess of approximately 3.2 standard deviations. Similarly, by examining other deviations from the SM, we observe a local data deficit of 2.5 standard deviations in the $10 < M_{\text{OSSF}}^{20} < 15\,\text{GeV}$ bin of the 3L(ee) 0B $400 < S_T < 800\,\text{GeV}$ channel (Fig. 5), and a local data excess of 2.5 standard deviations in the $60 < M_{\text{OSSF}}^{20} < 65\,\text{GeV}$ bin of the 3L($\mu\mu$) 1B $400 < S_T < 800\,\text{GeV}$ channel (Fig. 9). Other deviations are less significant. Overall, the observations are found to be globally consistent with the SM predictions within 2.7 standard deviations, and no statistically significant excess compatible with the signal models probed is observed.

Upper limits at 95% confidence level (CL) are set on the product of the signal production cross sections and branching fractions using a modified frequentist approach with the CL_s criterion [63, 64] and the asymptotic approximation for the test statistic [65, 66]. Upper limits at 95% CL are also set on the product of the branching fractions and the square of the scalar or pseudoscalar Yukawa coupling in the $t\bar{t}\phi$ model. A binned maximum-likelihood fit is performed to discriminate between the potential signal and the SM background processes for both signal models separately. All of the $L_T+p_T^{\text{miss}}$ and M_T bins are used for the seesaw signal masses under consideration, whereas the appropriate subset of the lepton flavor and dilepton mass bins is used for a given ϕ mass and branching fraction scenario in the $t\bar{t}\phi$ signal model, such that the low (high) dielectron and dimuon mass spectra are considered for a light (heavy) $t\bar{t}\phi$ signal with the $\phi \to \text{ee}$ and $\phi \to \mu\mu$ decays, respectively.

The uncertainties in the mean values of both the expected signal and background yields are treated as nuisance parameters modeled by log-normal and gamma distributions for systematic and statistical uncertainties, respectively. Statistical uncertainties in the signal and background yields in each bin and year are assumed to be fully uncorrelated, whereas all systematic uncertainties are assumed to be fully correlated among the signal bins in a given year. The correlation model of all nuisance parameters across the datasets collected in different years is summarized in Table 3.

The observed and expected upper limits on the production cross section $\sigma(\Sigma\Sigma)$ in the type-III seesaw signal model are given in Fig. 11. Type-III seesaw heavy fermions are excluded at 95% CL with masses below 880 GeV assuming the flavor-democratic scenario. Similarly, the upper limits on $\sigma(t\bar{t}\phi)\mathcal{B}(\phi \to \text{ee}/\mu\mu)$ and $g_t^2\mathcal{B}(\phi \to \text{ee}/\mu\mu)$ in the $t\bar{t}\phi$ signal model are shown in Figs. 12 and 13, respectively. In the $t\bar{t}\phi$ signal model, we exclude cross sections above 1–20 fb for ϕ masses in the range of 15–75 GeV, and above 0.3–5 fb for ϕ masses in the range of 108–340 GeV. Furthermore, $g_t^2\mathcal{B}(\phi \to \text{ee}/\mu\mu)$ above (0.4–4)$\times10^{-3}$ for the scalar and above (0.4–3)$\times10^{-2}$ for the pseudoscalar scenarios are excluded for ϕ masses in the 15–75 GeV range, whereas the two models perform similarly for masses 108–340 GeV and are excluded above (0.4–4)$\times10^{-2}$ for the scalar and above (0.6–3)$\times10^{-2}$ for the pseudoscalar scenarios. Uncertainties in the production cross sections due to scale and PDF choices are considered for both signal models [36, 37, 67], and are also shown in Figs. 11 and 12.

The differences in the low-mass exclusion limits of scalar and pseudoscalar $t\bar{t}\phi$ models result from the kinematic structure of the couplings, which affect both the production cross section and the signal efficiency of the ϕ bosons. The coupling of a scalar boson to a fermion is momentum independent, whereas that of a pseudoscalar boson is proportional to the momentum

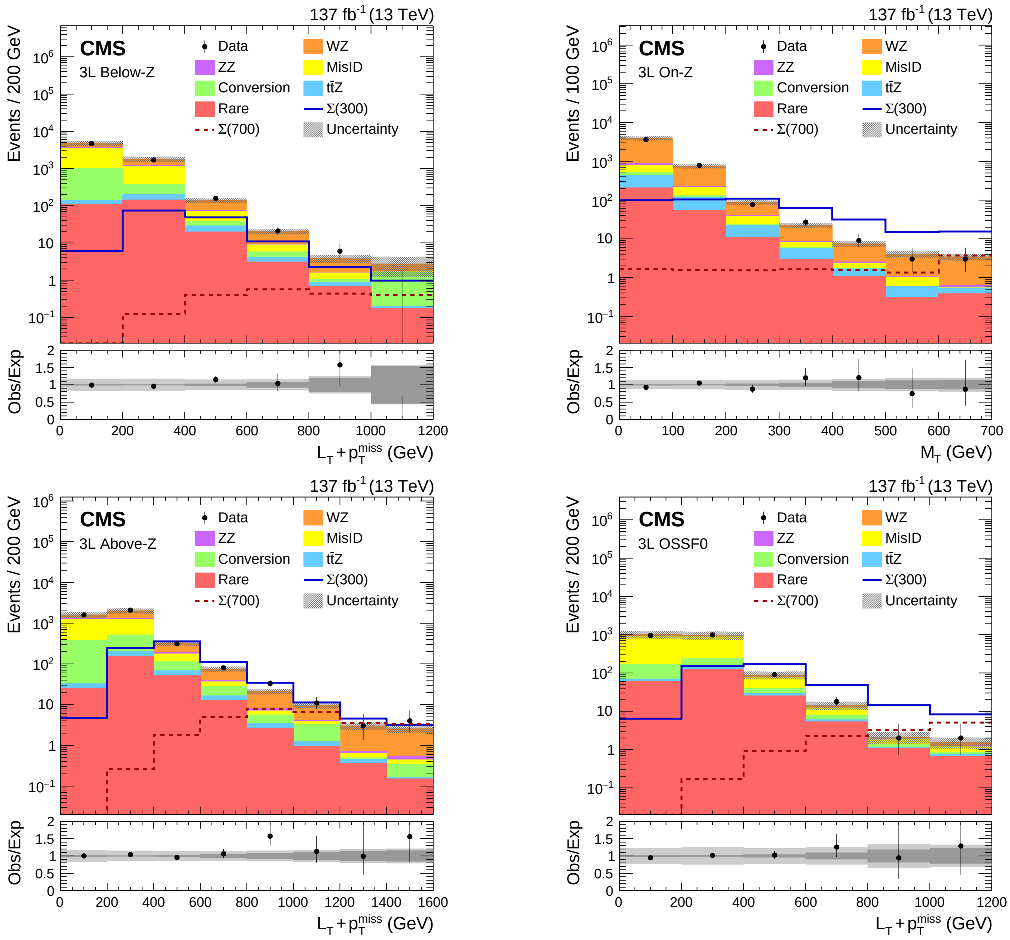

Figure 3: Type-III seesaw signal regions in 3L below-Z (upper left), on-Z (upper right), above-Z (lower left), and OSSF0 (lower right) events. The total SM background is shown as a stacked histogram of all contributing processes. The predictions for type-III seesaw models with Σ masses of 300 and 700 GeV in the flavor-democratic scenario are also shown. The lower panels show the ratio of observed to expected events. The hatched gray bands in the upper panels and the light gray bands in the lower panels represent the total (systematic and statistical) uncertainty of the backgrounds in each bin, whereas the dark gray bands in the lower panels represent only the statistical uncertainty of the backgrounds. The rightmost bins contain the overflow events in each distribution.

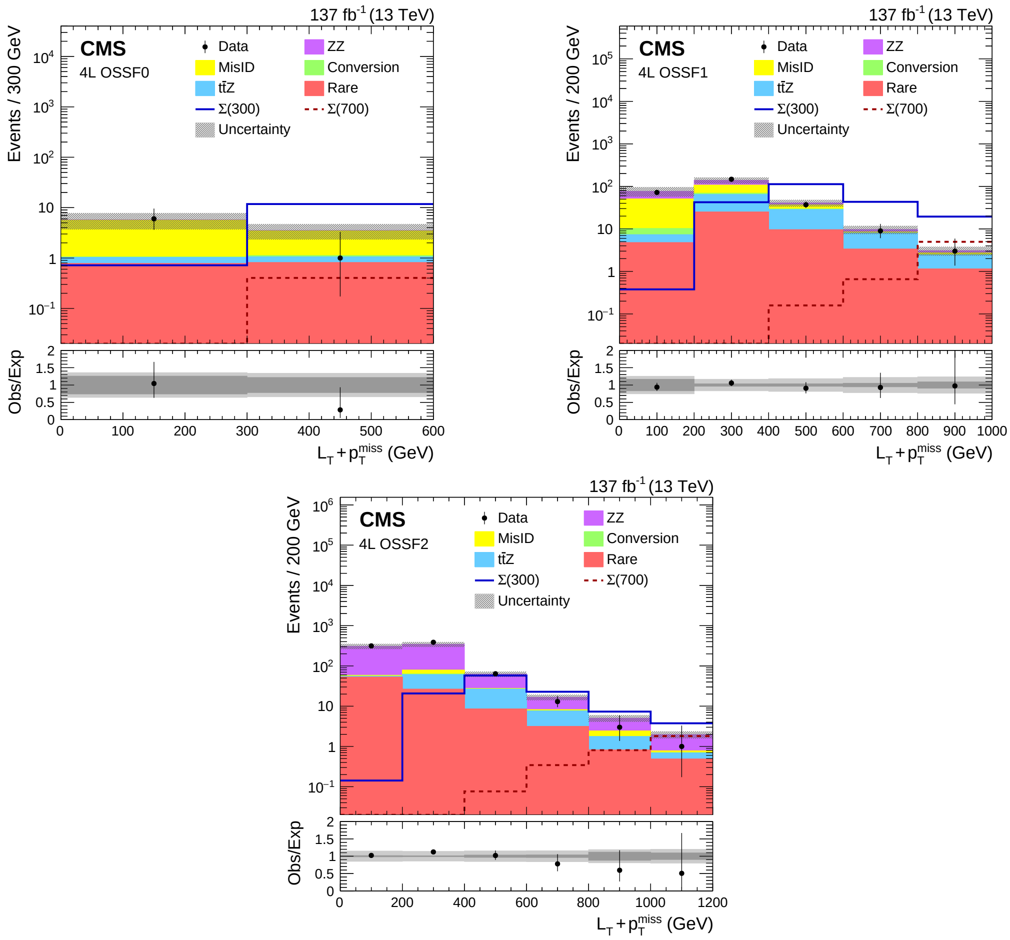

Figure 4: Type-III seesaw signal regions in 4L OSSF0 (upper left), OSSF1 (upper right), and OSSF2 (lower) events. The total SM background is shown as a stacked histogram of all contributing processes. The predictions for type-III seesaw models with Σ masses of 300 and 700 GeV in the flavor-democratic scenario are also shown. The lower panels show the ratio of observed to expected events. The hatched gray bands in the upper panels and the light gray bands in the lower panels represent the total (systematic and statistical) uncertainty of the backgrounds in each bin, whereas the dark gray bands in the lower panels represent only the statistical uncertainty of the backgrounds. The rightmost bins contain the overflow events in each distribution.

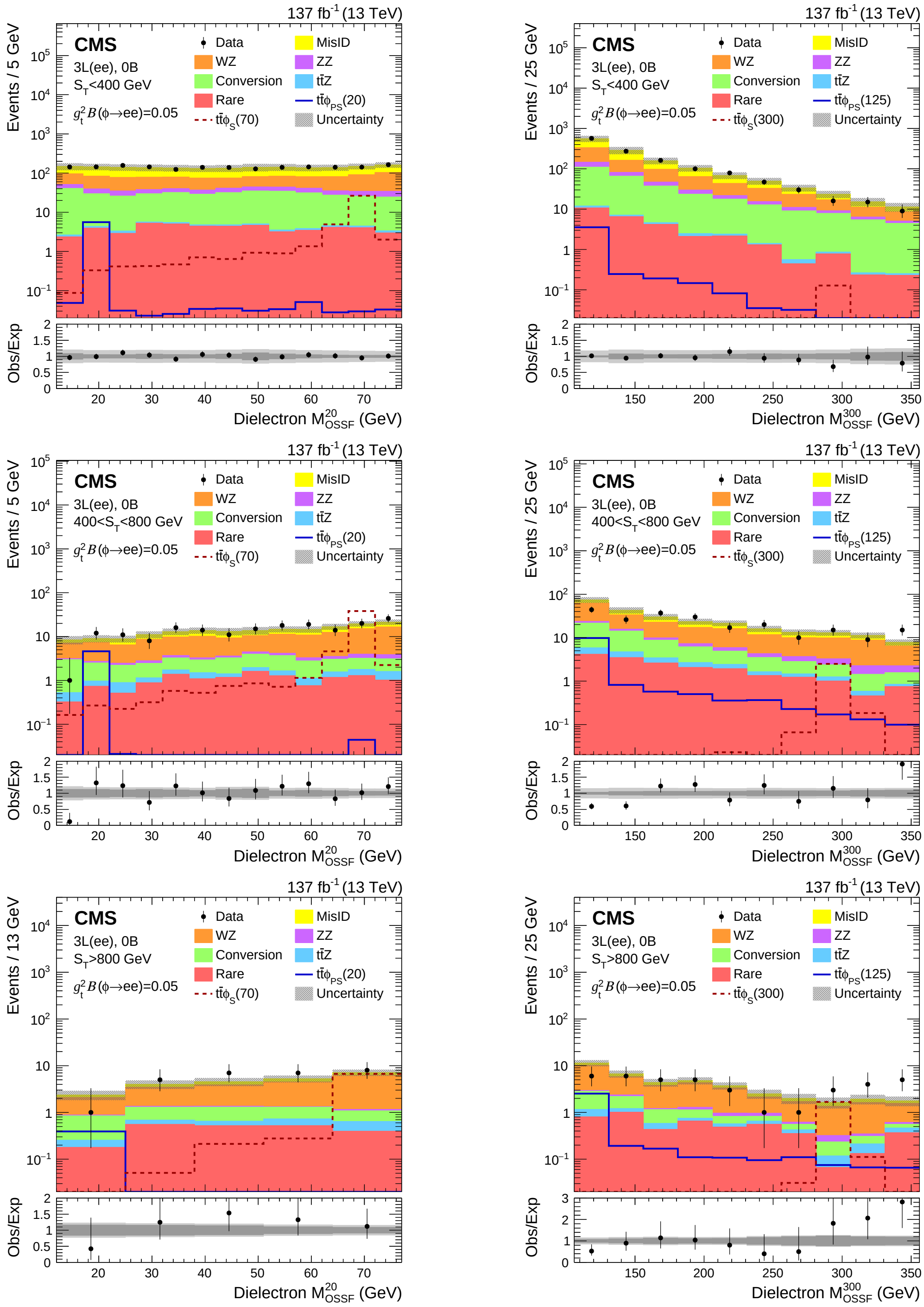

Figure 5: Dielectron M_{OSSF}^{20} (left column) and M_{OSSF}^{300} (right column) distributions in the 3L(ee) 0B $\mathrm{t\bar{t}}\phi$ signal regions. Upper, center, and lower plots are for $S_{\mathrm{T}} < 400\,\mathrm{GeV}$, $400 < S_{\mathrm{T}} < 800\,\mathrm{GeV}$, and $S_{\mathrm{T}} > 800\,\mathrm{GeV}$, respectively. The total SM background is shown as a stacked histogram of all contributing processes. The predictions for $\mathrm{t\bar{t}}\phi(\rightarrow \mathrm{ee})$ models with a pseudoscalar (scalar) ϕ of 20 and 125 (70 and 300) GeV mass assuming $g_{\mathrm{t}}^2\mathcal{B}(\phi \rightarrow \mathrm{ee}) = 0.05$ are also shown. The lower panels show the ratio of observed to expected events. The hatched gray bands in the upper panels and the light gray bands in the lower panels represent the total (systematic and statistical) uncertainty of the backgrounds in each bin, whereas the dark gray bands in the lower panels represent only the statistical uncertainty of the backgrounds. The rightmost bins do not contain the overflow events as these are outside the probed mass ranges.

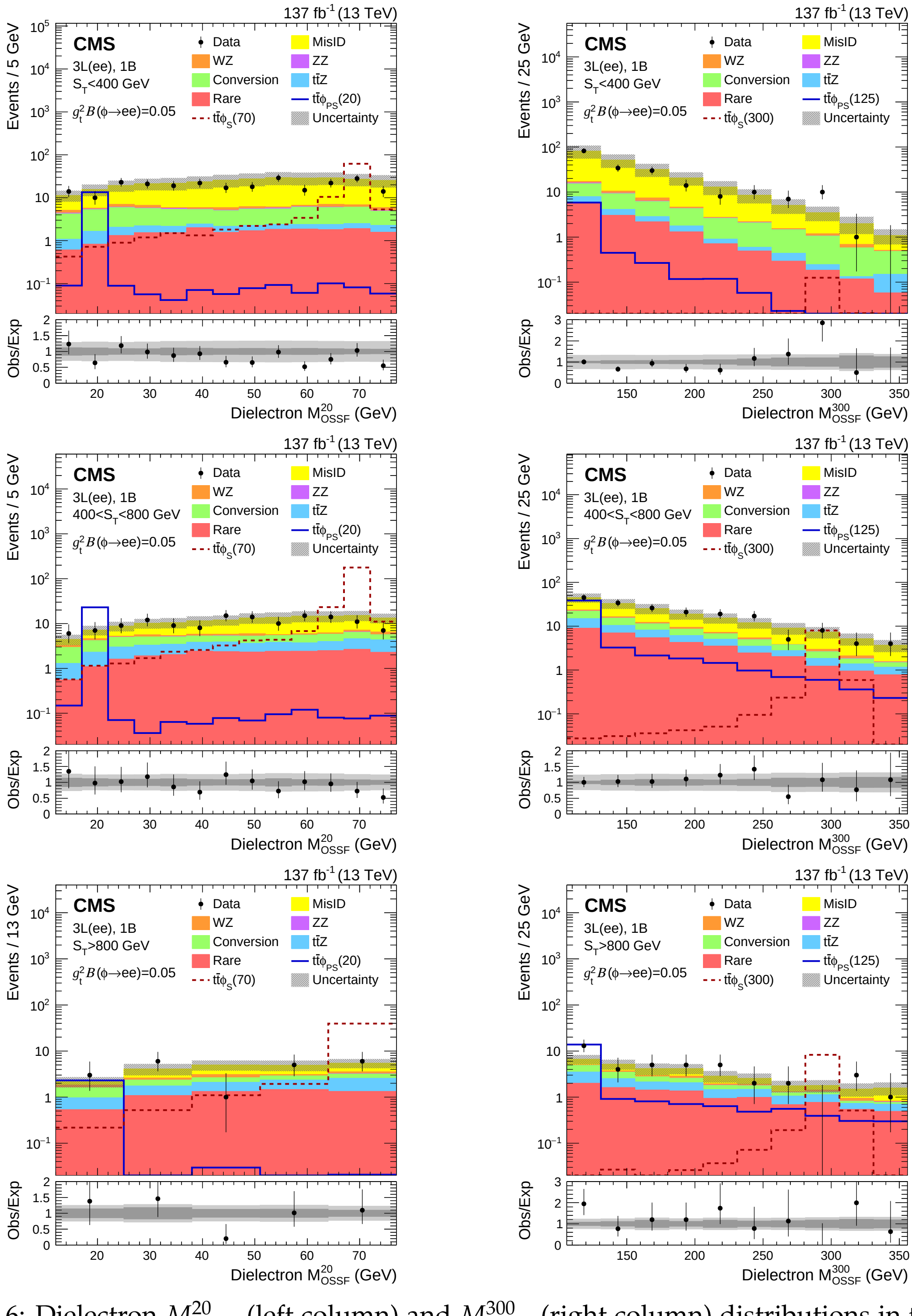

Figure 6: Dielectron M_{OSSF}^{20} (left column) and M_{OSSF}^{300} (right column) distributions in the 3L(ee) 1B $\mathrm{t\bar{t}}\phi$ signal regions. Upper, center, and lower plots are for $S_{\mathrm{T}} < 400\,\mathrm{GeV}$, $400 < S_{\mathrm{T}} < 800\,\mathrm{GeV}$, and $S_{\mathrm{T}} > 800\,\mathrm{GeV}$, respectively. The total SM background is shown as a stacked histogram of all contributing processes. The predictions for $\mathrm{t\bar{t}}\phi(\rightarrow \mathrm{ee})$ models with a pseudoscalar (scalar) ϕ of 20 and 125 (70 and 300) GeV mass assuming $g_{\mathrm{t}}^2\mathcal{B}(\phi \rightarrow \mathrm{ee}) = 0.05$ are also shown. The lower panels show the ratio of observed to expected events. The hatched gray bands in the upper panels and the light gray bands in the lower panels represent the total (systematic and statistical) uncertainty of the backgrounds in each bin, whereas the dark gray bands in the lower panels represent only the statistical uncertainty of the backgrounds. The rightmost bins do not contain the overflow events as these are outside the probed mass ranges.

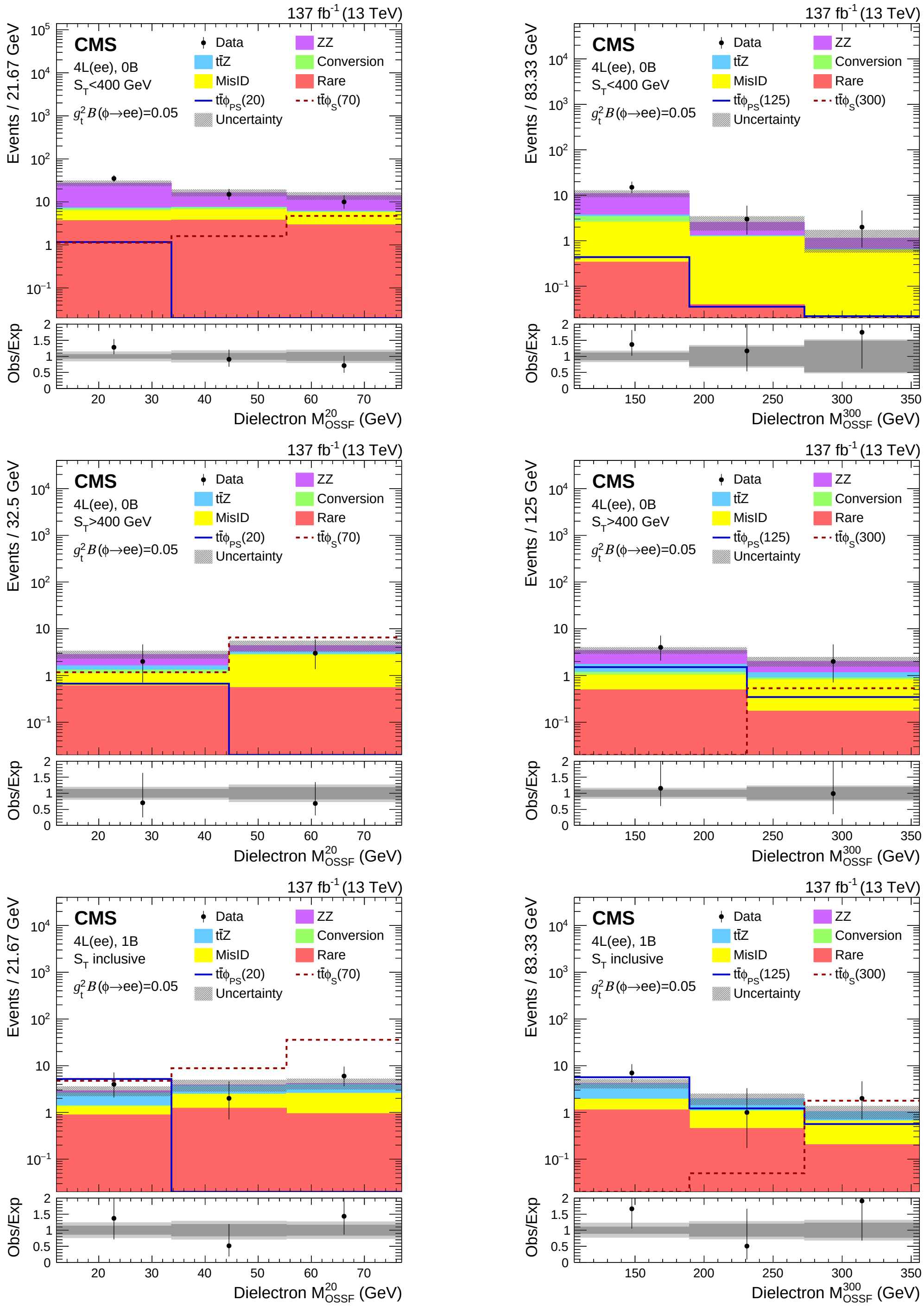

Figure 7: Dielectron M_{OSSF}^{20} (left column) and M_{OSSF}^{300} (right column) distributions in the 4L(ee) $\mathrm{t\bar{t}}\phi$ signal regions. Upper, center, and lower plots are for 0B $S_{\mathrm{T}} < 400\,\mathrm{GeV}$, 0B $S_{\mathrm{T}} > 400\,\mathrm{GeV}$, and 1B S_{T}-inclusive, respectively. The total SM background is shown as a stacked histogram of all contributing processes. The predictions for $\mathrm{t\bar{t}}\phi(\rightarrow \mathrm{ee})$ models with a pseudoscalar (scalar) ϕ of 20 and 125 (70 and 300) GeV mass assuming $g_{\mathrm{t}}^2\mathcal{B}(\phi \rightarrow \mathrm{ee}) = 0.05$ are also shown. The lower panels show the ratio of observed to expected events. The hatched gray bands in the upper panels and the light gray bands in the lower panels represent the total (systematic and statistical) uncertainty of the backgrounds in each bin, whereas the dark gray bands in the lower panels represent only the statistical uncertainty of the backgrounds. The rightmost bins do not contain the overflow events as these are outside the probed mass range.

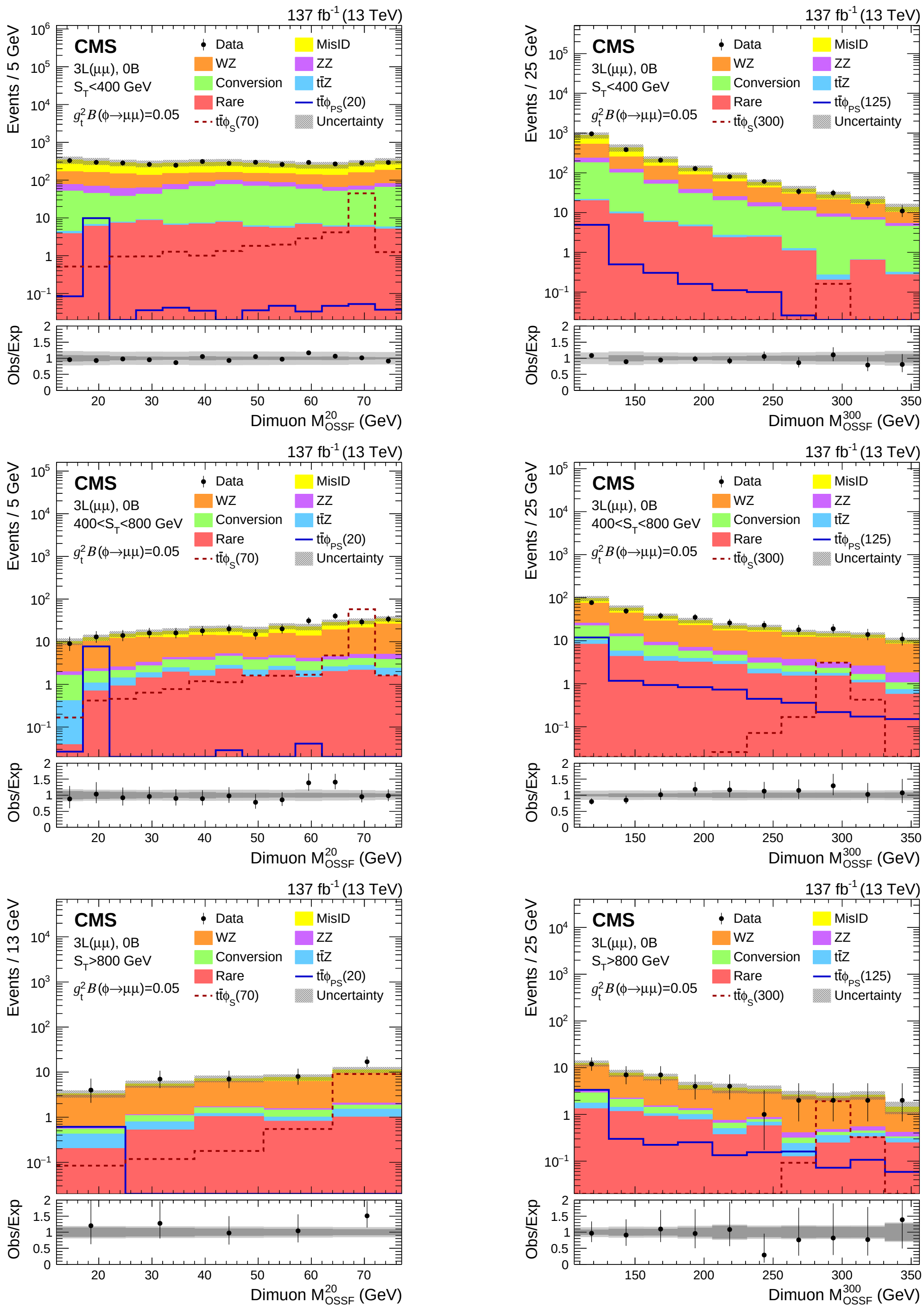

Figure 8: Dimuon M^{20}_{OSSF} (left column) and M^{300}_{OSSF} (right column) distributions in the 3L($\mu\mu$) 0B $\mathrm{t\bar{t}}\phi$ signal regions. Upper, center, and lower plots are for $S_{\mathrm{T}} < 400\,\mathrm{GeV}$, $400 < S_{\mathrm{T}} < 800\,\mathrm{GeV}$, and $S_{\mathrm{T}} > 800\,\mathrm{GeV}$, respectively. The total SM background is shown as a stacked histogram of all contributing processes. The predictions for $\mathrm{t\bar{t}}\phi(\to \mu\mu)$ models with a pseudoscalar (scalar) ϕ of 20 and 125 (70 and 300) GeV mass assuming $g_{\mathrm{t}}^2\mathcal{B}(\phi \to \mu\mu) = 0.05$ are also shown. The lower panels show the ratio of observed to expected events. The hatched gray bands in the upper panels and the light gray bands in the lower panels represent the total (systematic and statistical) uncertainty of the backgrounds in each bin, whereas the dark gray bands in the lower panels represent only the statistical uncertainty of the backgrounds. The rightmost bins do not contain the overflow events as these are outside the probed mass range.

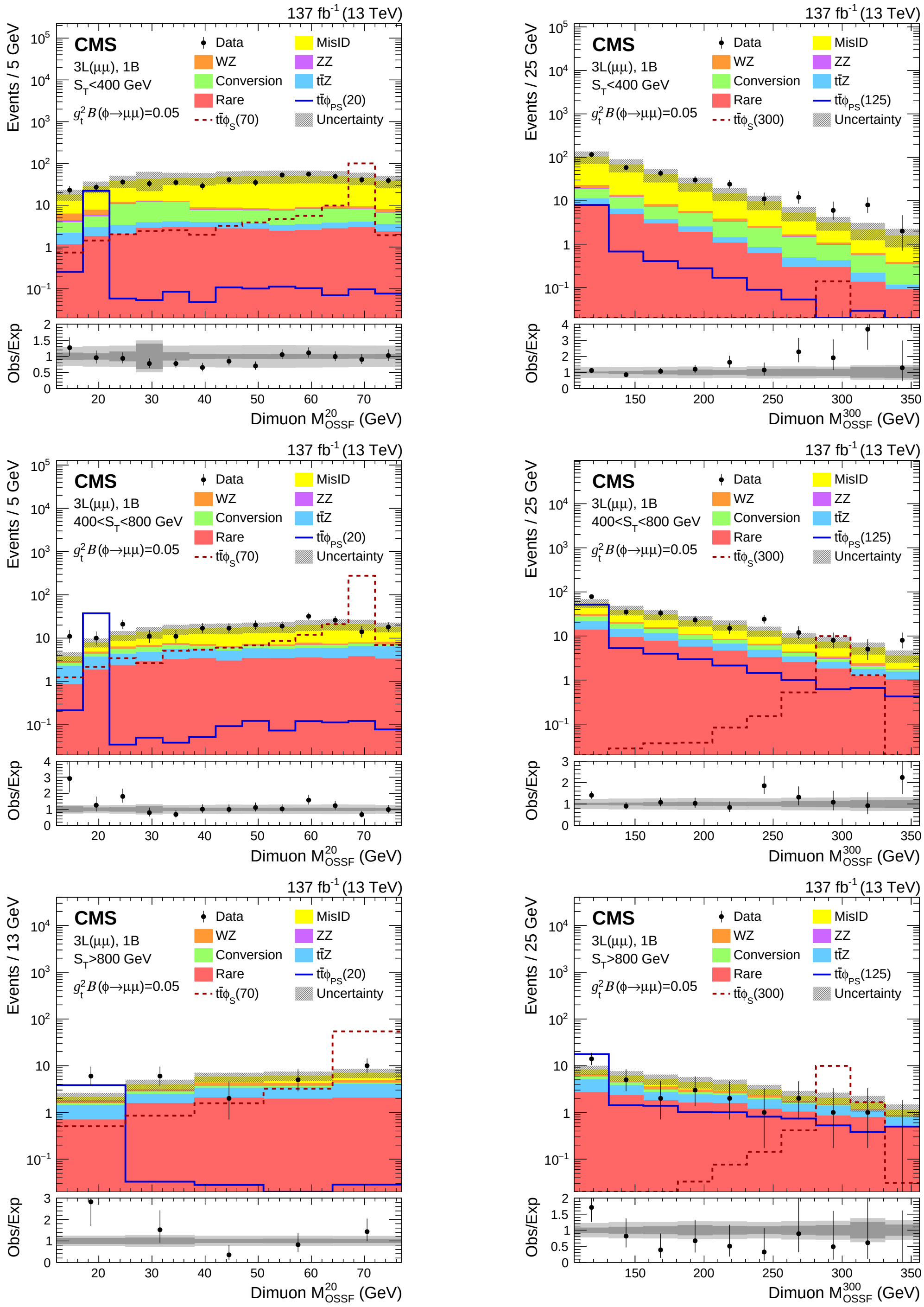

Figure 9: Dimuon M^{20}_{OSSF} (left column) and M^{300}_{OSSF} (right column) distributions in the 3L($\mu\mu$) 1B $\mathrm{t\bar{t}}\phi$ signal regions. Upper, center, and lower plots are for $S_{\mathrm{T}} < 400\,\mathrm{GeV}$, $400 < S_{\mathrm{T}} < 800\,\mathrm{GeV}$, and $S_{\mathrm{T}} > 800\,\mathrm{GeV}$, respectively. The total SM background is shown as a stacked histogram of all contributing processes. The predictions for $\mathrm{t\bar{t}}\phi(\rightarrow \mu\mu)$ models with a pseudoscalar (scalar) ϕ of 20 and 125 (70 and 300) GeV mass assuming $g_{\mathrm{t}}^2\mathcal{B}(\phi \rightarrow \mu\mu) = 0.05$ are also shown. The lower panels show the ratio of observed to expected events. The hatched gray bands in the upper panels and the light gray bands in the lower panels represent the total (systematic and statistical) uncertainty of the backgrounds in each bin, whereas the dark gray bands in the lower panels represent only the statistical uncertainty of the backgrounds. The rightmost bins do not contain the overflow events as these are outside the probed mass range.

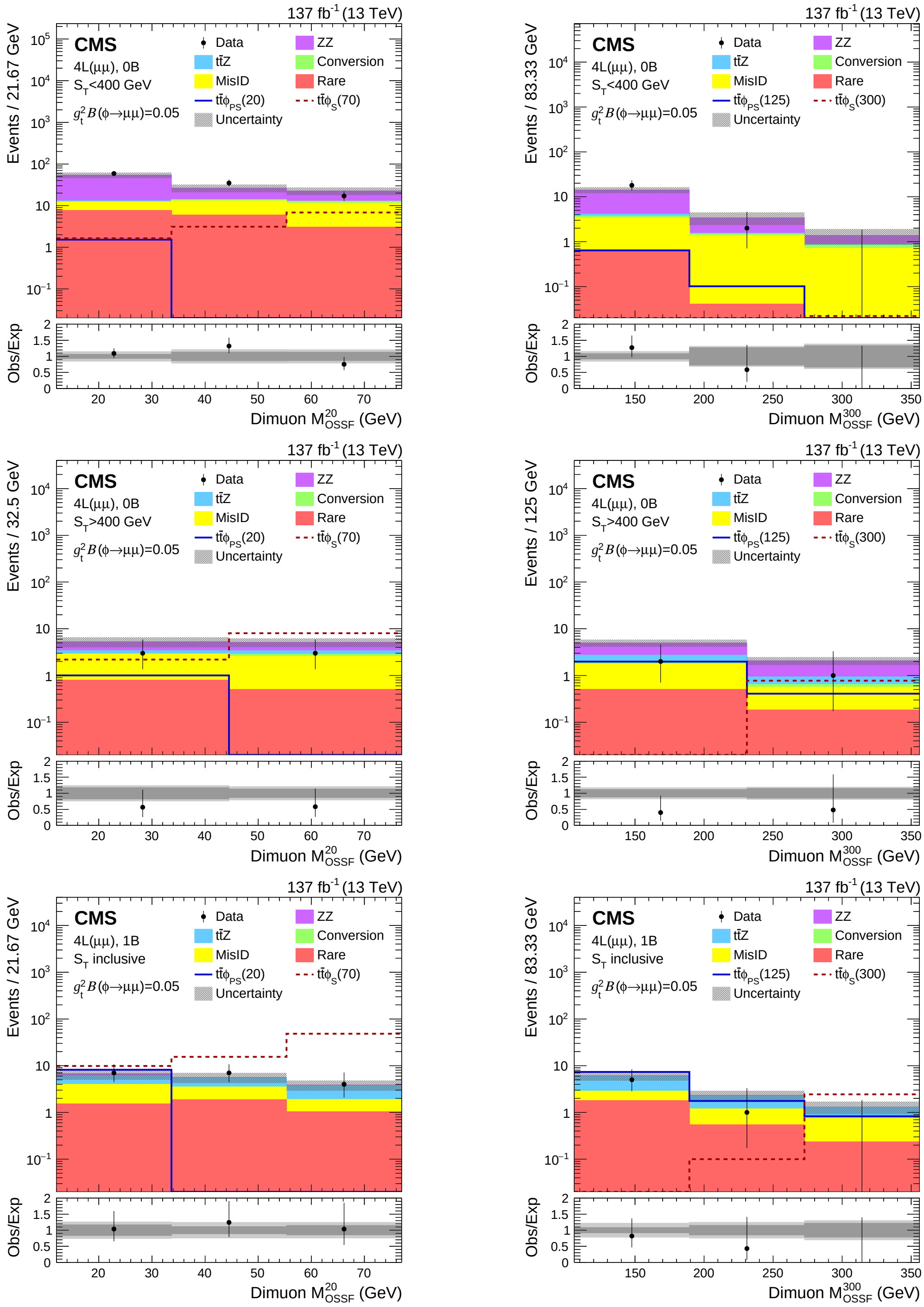

Figure 10: Dimuon M_{OSSF}^{20} (left column) and M_{OSSF}^{300} (right column) distributions in the 4L($\mu\mu$) $\mathrm{t\bar{t}}\phi$ signal regions. Upper, center, and lower plots are for 0B $S_{\mathrm{T}} < 400\,\mathrm{GeV}$, 0B $S_{\mathrm{T}} > 400\,\mathrm{GeV}$, and 1B S_{T}-inclusive, respectively. The total SM background is shown as a stacked histogram of all contributing processes. The predictions for $\mathrm{t\bar{t}}\phi(\rightarrow \mu\mu)$ models with a pseudoscalar (scalar) ϕ of 20 and 125 (70 and 300) GeV mass assuming $g_{\mathrm{t}}^2\mathcal{B}(\phi \rightarrow \mu\mu) = 0.05$ are also shown. The lower panels show the ratio of observed to expected events. The hatched gray bands in the upper panels and the light gray bands in the lower panels represent the total (systematic and statistical) uncertainty of the backgrounds in each bin, whereas the dark gray bands in the lower panels represent only the statistical uncertainty of the backgrounds. The rightmost bins do not contain the overflow events as these are outside the probed mass range.

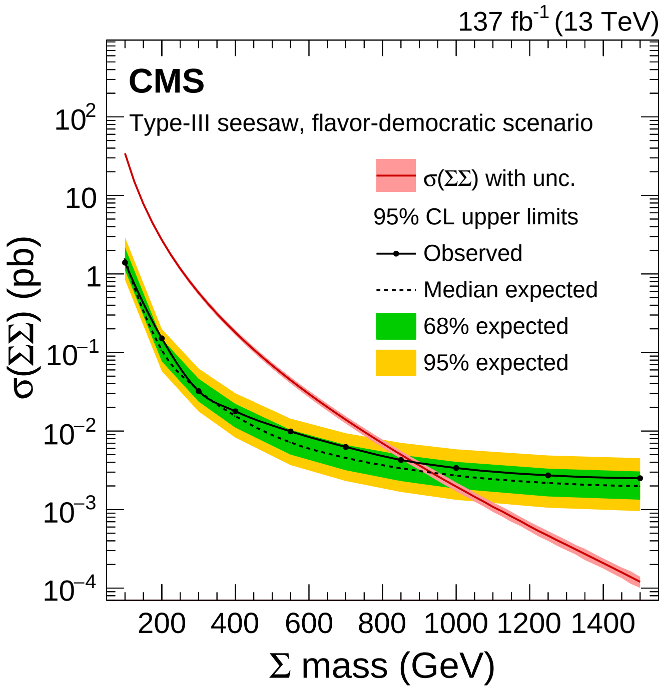

Figure 11: The 95% confidence level expected and observed upper limits on the total production cross section of heavy fermion pairs. The inner (green) and the outer (yellow) bands indicate the regions containing 68 and 95%, respectively, of the distribution of limits expected under the background-only hypothesis. Also shown are the theoretical prediction for the cross section and the associated uncertainty of the Σ pair production via the type-III seesaw mechanism. Type-III seesaw heavy fermions are excluded for masses below 880 GeV (expected limit 930 GeV) in the flavor-democratic scenario.

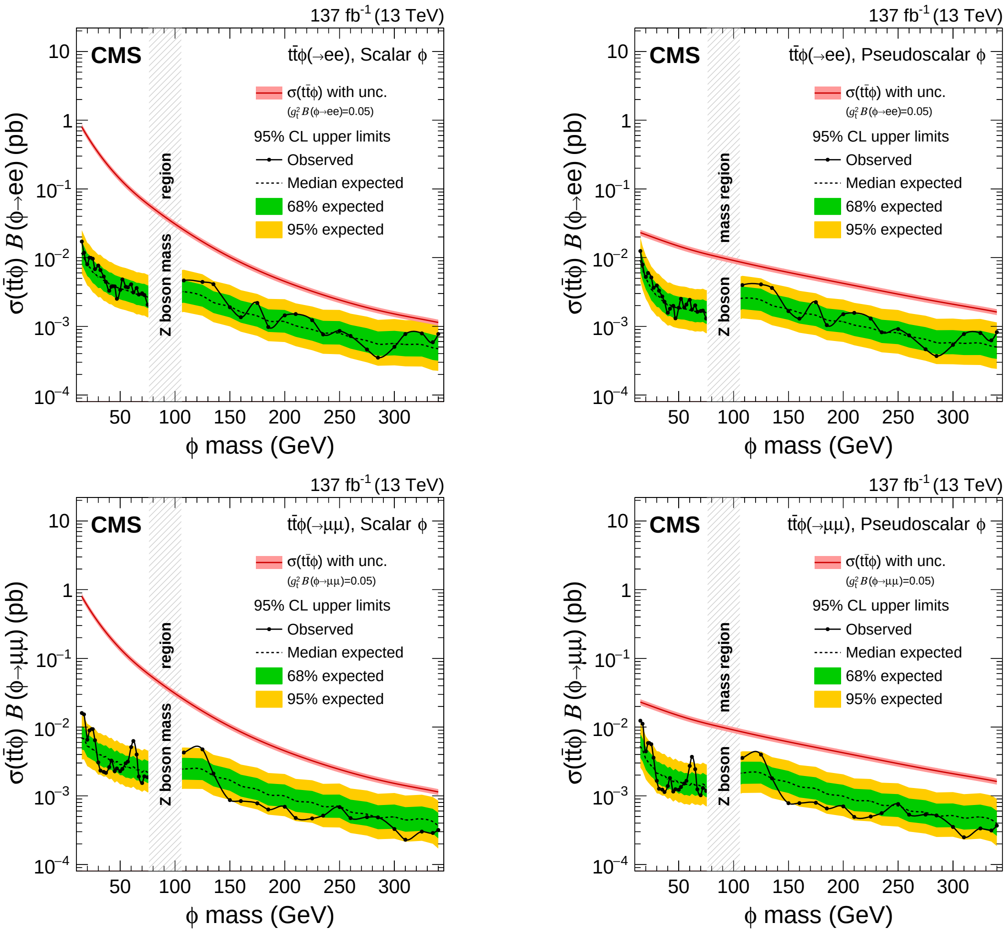

Figure 12: The 95% confidence level expected and observed upper limits on the product of the signal production cross section and branching fraction of a scalar ϕ boson in the dielectron (upper left) and dimuon (lower left) channels, and of a pseudoscalar ϕ boson in the dielectron (upper right) and dimuon (lower right) channels, where ϕ is produced in association with a top quark pair. The inner (green) and the outer (yellow) bands indicate the regions containing 68 and 95%, respectively, of the distribution of limits expected under the background-only hypothesis. The vertical hatched gray band indicates the mass region corresponding to the Z boson veto. Also shown are the theoretical predictions for the product of the production cross section and branching fraction of the $t\bar{t}\phi$ model, with their uncertainties, and assuming $g_t^2\mathcal{B}(\phi \to ee/\mu\mu) = 0.05$. All $t\bar{t}\phi$ signal scenarios are excluded for the product of the production cross section and branching fraction above 1–20 fb for ϕ masses in the range of 15–75 GeV, and above 0.3–5 fb for ϕ masses in the range of 108–340 GeV.

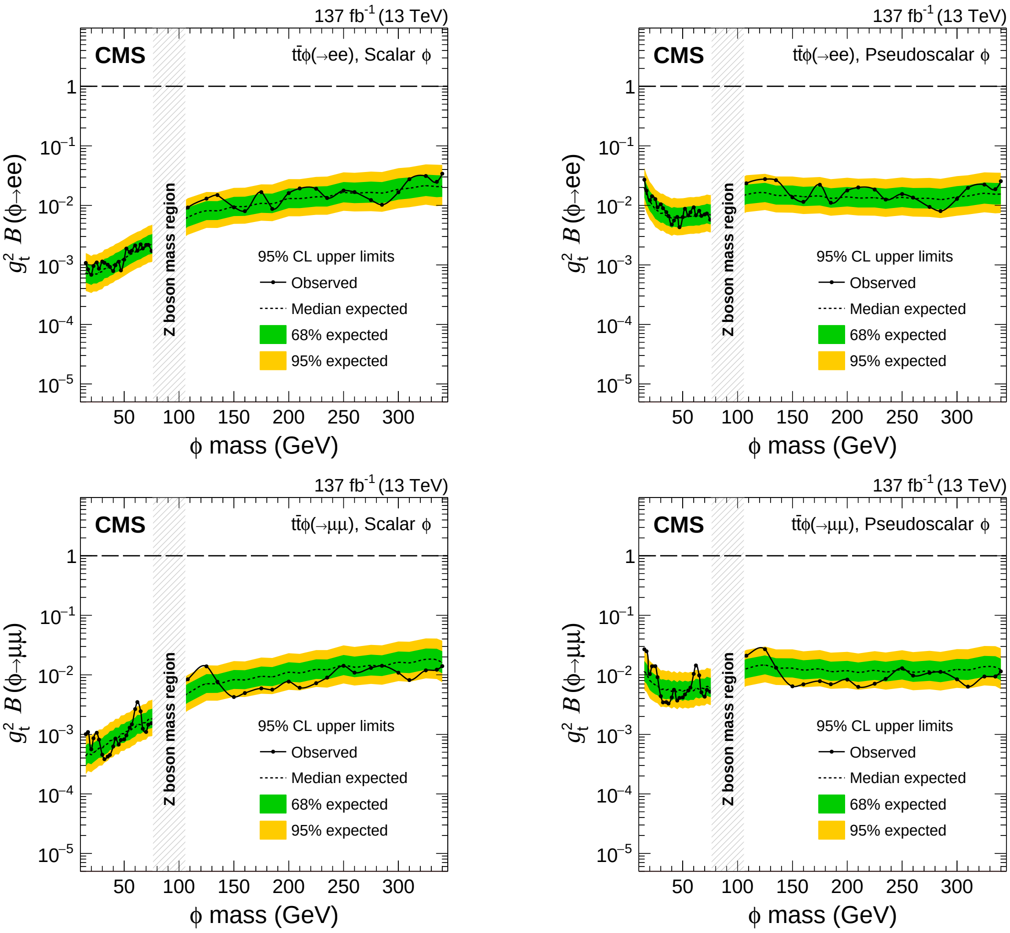

Figure 13: The 95% confidence level expected and observed upper limits on the product of the square of the Yukawa coupling to top quarks and branching fraction of a scalar ϕ boson in the dielectron (upper left) and dimuon (lower left) channels, and of a pseudoscalar ϕ boson in the dielectron (upper right) and dimuon (lower right) channels, where ϕ is produced in association with a top quark pair. The inner (green) and the outer (yellow) bands indicate the regions containing 68 and 95%, respectively, of the distribution of limits expected under the background-only hypothesis. The vertical hatched gray band indicates the mass region corresponding to the Z boson veto. The dashed horizontal line marks the unity value of the product of the square of the Yukawa coupling to top quarks and the branching fraction. Assuming a Yukawa coupling of unit strength to top quarks, the branching fraction of new scalar (pseudoscalar) bosons to dielectrons or dimuons above 0.0004–0.004 (0.004–0.03) are excluded for masses in the range of 15–75 GeV, and above 0.004–0.04 (0.006–0.03) for masses in the range of 108–340 GeV.

in the low momentum limit. Therefore, the low ϕ momentum part of the production cross section is suppressed in the pseudoscalar model in comparison to the scalar model for ϕ masses below the top quark mass scale, while both production cross sections are similar for ϕ masses at and above the top quark mass scale. Furthermore, this coupling structure results in more pseudoscalar ϕ bosons in the Lorentz-boosted region compared to the scalar ϕ bosons, yielding more energetic leptons with higher selection efficiencies. The product of the fiducial acceptance and the event selection efficiency for the type-III seesaw and the $t\bar{t}\phi$ models for various signal mass hypotheses, calculated after all analysis selection requirements, are given in Table 4.

Table 4: Product of the fiducial acceptance and the event selection efficiency for the signal models at various signal mass hypotheses calculated after all analysis selection requirements.

Signal model	Product of acceptance and efficiency (%)														
Type-III seesaw (flavor-democratic scenario)															
Σ mass (GeV)	100	200	300	400	550	700	850	1000	1250	1500					
	0.32	1.82	2.63	3.02	3.29	3.34	3.29	3.21	2.99	2.82					
$t\bar{t}\phi$															
ϕ mass (GeV)	15	20	25	30	40	50	60	70	75	108	125	150	200	250	300
Scalar $\phi(\to ee)$	0.85	1.29	1.67	2.02	2.74	3.44	4.25	5.16	4.95	5.53	8.32	9.00	10.3	11.1	11.5
Scalar $\phi(\to \mu\mu)$	1.54	2.16	2.81	3.35	4.38	5.29	6.40	7.69	7.56	8.74	11.6	12.3	14.0	14.8	15.3
Pseudoscalar $\phi(\to ee)$	0.96	1.81	2.69	3.45	4.88	5.82	6.62	7.35	6.83	6.8	9.77	10.4	11.0	11.4	11.9
Pseudoscalar $\phi(\to \mu\mu)$	1.69	2.95	4.24	5.38	7.14	8.46	9.73	10.4	9.93	10.3	13.4	14.0	14.9	15.2	15.9

8 Summary

A search has been performed for physics beyond the standard model, using multilepton events in 137 fb^{-1} of pp collision data at $\sqrt{s} = 13$ TeV, collected with the CMS detector in 2016–2018. The observations are found to be consistent with the expectations from standard model processes, with no statistically significant signal-like excess in any of the probed channels. The results are used to constrain the allowed parameter space of the targeted signal models. At 95% confidence level, heavy fermions of the type-III seesaw model with masses below 880 GeV are excluded assuming identical Σ decay branching fractions across all lepton flavors. This is the most restrictive limit on the flavor-democratic scenario of the type-III seesaw model to date. Assuming a Yukawa coupling of unit strength to top quarks, branching fractions of new scalar (pseudoscalar) bosons to dielectrons or dimuons above 0.004 (0.03) are excluded at 95% confidence level for masses in the range 15–75 GeV, and above 0.04 (0.03) for masses in the range 108–340 GeV. These are the first limits in these channels on an extension of the standard model with scalar or pseudoscalar particles.

Acknowledgments

We thank M. J. Strassler for drawing our attention to the need to include top quark pair production with three-body top quark decays, $t \to bW\phi$, in the $t\bar{t}\phi$ signal model.

We congratulate our colleagues in the CERN accelerator departments for the excellent performance of the LHC and thank the technical and administrative staffs at CERN and at other CMS institutes for their contributions to the success of the CMS effort. In addition, we gratefully acknowledge the computing centers and personnel of the Worldwide LHC Computing Grid for delivering so effectively the computing infrastructure essential to our analyses. Finally, we acknowledge the enduring support for the construction and operation of the LHC and the CMS detector provided by the following funding agencies: BMBWF and FWF (Austria); FNRS and FWO (Belgium); CNPq, CAPES, FAPERJ, FAPERGS, and FAPESP (Brazil); MES (Bulgaria); CERN; CAS, MoST, and NSFC (China); COLCIENCIAS (Colombia); MSES and CSF (Croatia); RPF (Cyprus); SENESCYT (Ecuador); MoER, ERC IUT, PUT and ERDF (Estonia); Academy of Finland, MEC, and HIP (Finland); CEA and CNRS/IN2P3 (France); BMBF, DFG, and HGF (Germany); GSRT (Greece); NKFIA (Hungary); DAE and DST (India); IPM (Iran); SFI (Ireland); INFN (Italy); MSIP and NRF (Republic of Korea); MES (Latvia); LAS (Lithuania); MOE and UM (Malaysia); BUAP, CINVESTAV, CONACYT, LNS, SEP, and UASLP-FAI (Mexico); MOS (Montenegro); MBIE (New Zealand); PAEC (Pakistan); MSHE and NSC (Poland); FCT (Portugal); JINR (Dubna); MON, RosAtom, RAS, RFBR, and NRC KI (Russia); MESTD (Serbia); SEIDI, CPAN, PCTI, and FEDER (Spain); MOSTR (Sri Lanka); Swiss Funding Agencies (Switzerland); MST (Taipei); ThEPCenter, IPST, STAR, and NSTDA (Thailand); TUBITAK and TAEK (Turkey); NASU (Ukraine); STFC (United Kingdom); DOE and NSF (USA).

Individuals have received support from the Marie-Curie program and the European Research Council and Horizon 2020 Grant, contract Nos. 675440, 752730, and 765710 (European Union); the Leventis Foundation; the A.P. Sloan Foundation; the Alexander von Humboldt Foundation; the Belgian Federal Science Policy Office; the Fonds pour la Formation à la Recherche dans l'Industrie et dans l'Agriculture (FRIA-Belgium); the Agentschap voor Innovatie door Wetenschap en Technologie (IWT-Belgium); the F.R.S.-FNRS and FWO (Belgium) under the "Excellence of Science – EOS" – be.h project n. 30820817; the Beijing Municipal Science & Technology Commission, No. Z181100004218003; the Ministry of Education, Youth and Sports (MEYS) of the Czech Republic; the Lendület ("Momentum") Program and the János Bolyai Research Scholarship of the Hungarian Academy of Sciences, the New National Excellence Program ÚNKP, the NKFIA research grants 123842, 123959, 124845, 124850, 125105, 128713, 128786, and 129058 (Hungary); the Council of Science and Industrial Research, India; the HOMING PLUS program of the Foundation for Polish Science, cofinanced from European Union, Regional Development Fund, the Mobility Plus program of the Ministry of Science and Higher Education, the National Science Center (Poland), contracts Harmonia 2014/14/M/ST2/00428, Opus 2014/13/B/ST2/02543, 2014/15/B/ST2/03998, and 2015/19/B/ST2/02861, Sonata-bis 2012/07/E/ST2/01406; the National Priorities Research Program by Qatar National Research Fund; the Ministry of Science and Education, grant no. 3.2989.2017 (Russia); the Programa Estatal de Fomento de la Investigación Científica y Técnica de Excelencia María de Maeztu, grant MDM-2015-0509 and the Programa Severo Ochoa del Principado de Asturias; the Thalis and Aristeia programs cofinanced by EU-ESF and the Greek NSRF; the Rachadapisek Sompot Fund for Postdoctoral Fellowship, Chulalongkorn University and the Chulalongkorn Academic into Its 2nd Century Project Advancement Project (Thailand); the Nvidia Corporation; the Welch Foundation, contract C-1845; and the Weston Havens Foundation (USA).

References

[1] P. Minkowski, "$\mu \to e\gamma$ at a rate of one out of 10^9 muon decays?", *Phys. Lett. B* **67** (1977) 421, doi:10.1016/0370-2693(77)90435-X.

[2] R. N. Mohapatra and G. Senjanovic, "Neutrino mass and spontaneous parity nonconservation", *Phys. Rev. Lett.* **44** (1980) 912, doi:10.1103/PhysRevLett.44.912.

[3] M. Magg and C. Wetterich, "Neutrino mass problem and gauge hierarchy", *Phys. Lett. B* **94** (1980) 61, doi:10.1016/0370-2693(80)90825-4.

[4] R. N. Mohapatra and G. Senjanovic, "Neutrino masses and mixings in gauge models with spontaneous parity violation", *Phys. Rev. D* **23** (1981) 165, doi:10.1103/PhysRevD.23.165.

[5] J. Schechter and J. W. F. Valle, "Neutrino masses in SU(2) x U(1) theories", *Phys. Rev. D* **22** (1980) 2227, doi:10.1103/PhysRevD.22.2227.

[6] J. Schechter and J. W. F. Valle, "Neutrino decay and spontaneous violation of lepton number", *Phys. Rev. D* **25** (1982) 774, doi:10.1103/PhysRevD.25.774.

[7] R. Foot, H. Lew, X. G. He, and G. C. Joshi, "Seesaw neutrino masses induced by a triplet of leptons", *Z. Phys. C* **44** (1989) 441, doi:10.1007/BF01415558.

[8] R. N. Mohapatra, "Mechanism for understanding small neutrino mass in superstring theories", *Phys. Rev. Lett.* **56** (1986) 561, doi:10.1103/PhysRevLett.56.561.

[9] R. N. Mohapatra and J. W. F. Valle, "Neutrino mass and baryon number nonconservation in superstring models", *Phys. Rev. D* **34** (1986) 1642, doi:10.1103/PhysRevD.34.1642.

[10] C. Biggio and F. Bonnet, "Implementation of the type-III seesaw model in FeynRules/MadGraph and prospects for discovery with early LHC data", *Eur. Phys. J. C* **72** (2012) 1899, doi:10.1140/epjc/s10052-012-1899-z, arXiv:1107.3463.

[11] A. Abada et al., "$\mu \to e\gamma$ and $\tau \to \ell\gamma$ decays in the fermion triplet seesaw model", *Phys. Rev. D* **78** (2008) 033007, doi:10.1103/PhysRevD.78.033007, arXiv:0803.0481.

[12] A. Abada et al., "Low energy effects of neutrino masses", *JHEP* **12** (2007) 061, doi:10.1088/1126-6708/2007/12/061, arXiv:0707.4058.

[13] F. del Aguila, J. de Blas, and M. Perez-Victoria, "Effects of new leptons in electroweak precision data", *Phys. Rev. D* **78** (2008) 013010, doi:10.1103/PhysRevD.78.013010, arXiv:0803.4008.

[14] D. Goswami and P. Poulose, "Direct searches of type-III seesaw triplet fermions at high energy e^+e^- collider", *Eur. Phys. J. C* **78** (2018) 42, doi:10.1140/epjc/s10052-017-5478-1, arXiv:1702.07215.

[15] G. Cacciapaglia, G. Ferretti, T. Flacke, and H. Serodio, "Light scalars in composite Higgs models", *Front. Phys.* **7** (2019) 22, doi:10.3389/fphy.2019.00022, arXiv:1902.06890.

[16] U. Ellwanger, C. Hugonie, and A. M. Teixeira, "The next-to-minimal supersymmetric standard model", *Phys. Rept.* **496** (2010) 1, doi:10.1016/j.physrep.2010.07.001, arXiv:0910.1785.

[17] M. Maniatis, "The next-to-minimal supersymmetric extension of the standard model reviewed", *Int. J. Mod. Phys. A* **25** (2010) 3505, doi:10.1142/S0217751X10049827, arXiv:0906.0777.

[18] M. R. Buckley, D. Feld, and D. Goncalves, "Scalar simplified models for dark matter", *Phys. Rev. D* **91** (2015) 015017, doi:10.1103/PhysRevD.91.015017, arXiv:1410.6497.

[19] M. Casolino et al., "Probing a light CP-odd scalar in di-top-associated production at the LHC", *Eur. Phys. J. C* **75** (2015) 498, doi:10.1140/epjc/s10052-015-3708-y, arXiv:1507.07004.

[20] W.-F. Chang, T. Modak, and J. N. Ng, "Signal for a light singlet scalar at the LHC", *Phys. Rev. D* **97** (2018) 055020, doi:10.1103/PhysRevD.97.055020, arXiv:1711.05722.

[21] CMS Collaboration, "Search for heavy lepton partners of neutrinos in proton-proton collisions in the context of the type-III seesaw mechanism", *Phys. Lett. B* **718** (2012) 348, doi:10.1016/j.physletb.2012.10.070, arXiv:1210.1797.

[22] ATLAS Collaboration, "Search for type-III seesaw heavy leptons in pp collisions at $\sqrt{s} = 8$ TeV with the ATLAS detector", *Phys. Rev. D* **92** (2015) 032001, doi:10.1103/PhysRevD.92.032001, arXiv:1506.01839.

[23] ATLAS Collaboration, "Search for heavy lepton resonances decaying to a Z boson and a lepton in pp collisions at $\sqrt{s} = 8$ TeV with the ATLAS detector", *JHEP* **09** (2015) 108, doi:10.1007/JHEP09(2015)108, arXiv:1506.01291.

[24] CMS Collaboration, "Search for evidence of the type-III seesaw mechanism in multilepton final states in proton-proton collisions at $\sqrt{s} = 13$ TeV", *Phys. Rev. Lett.* **119** (2017) 221802, doi:10.1103/PhysRevLett.119.221802, arXiv:1708.07962.

[25] CMS Collaboration, "The CMS experiment at the CERN LHC", *JINST* **3** (2008) S08004, doi:10.1088/1748-0221/3/08/S08004.

[26] CMS Collaboration, "The CMS trigger system", *JINST* **12** (2017) P01020, doi:10.1088/1748-0221/12/01/P01020, arXiv:1609.02366.

[27] J. Alwall et al., "The automated computation of tree-level and next-to-leading order differential cross sections, and their matching to parton shower simulations", *JHEP* **07** (2014) 079, doi:10.1007/JHEP07(2014)079, arXiv:1405.0301.

[28] P. Nason, "A new method for combining NLO QCD with shower Monte Carlo algorithms", *JHEP* **11** (2004) 040, doi:10.1088/1126-6708/2004/11/040, arXiv:hep-ph/0409146.

[29] S. Frixione, P. Nason, and C. Oleari, "Matching NLO QCD computations with parton shower simulations: the POWHEG method", *JHEP* **11** (2007) 070, doi:10.1088/1126-6708/2007/11/070, arXiv:0709.2092.

[30] S. Alioli, P. Nason, C. Oleari, and E. Re, "A general framework for implementing NLO calculations in shower Monte Carlo programs: the POWHEG BOX", *JHEP* **06** (2010) 043, doi:10.1007/JHEP06(2010)043, arXiv:1002.2581.

[31] J. M. Campbell and R. K. Ellis, "MCFM for the Tevatron and the LHC", *Nucl. Phys. Proc. Suppl.* **205–206** (2010) 10, doi:10.1016/j.nuclphysbps.2010.08.011, arXiv:1007.3492.

[32] Y. Gao et al., "Spin determination of single-produced resonances at hadron colliders", *Phys. Rev. D* **81** (2010) 075022, doi:10.1103/PhysRevD.81.075022, arXiv:1001.3396.

[33] S. Bolognesi et al., "On the spin and parity of a single-produced resonance at the LHC", *Phys. Rev. D* **86** (2012) 095031, doi:10.1103/PhysRevD.86.095031, arXiv:1208.4018.

[34] I. Anderson et al., "Constraining anomalous HVV interactions at proton and lepton colliders", *Phys. Rev. D* **89** (2014) 035007, doi:10.1103/PhysRevD.89.035007, arXiv:1309.4819.

[35] A. V. Gritsan, R. Röntsch, M. Schulze, and M. Xiao, "Constraining anomalous Higgs boson couplings to the heavy flavor fermions using matrix element techniques", *Phys. Rev. D* **94** (2016) 055023, doi:10.1103/PhysRevD.94.055023, arXiv:1606.03107.

[36] B. Fuks, M. Klasen, D. R. Lamprea, and M. Rothering, "Gaugino production in proton-proton collisions at a center-of-mass energy of 8 TeV", *JHEP* **10** (2012) 081, doi:10.1007/JHEP10(2012)081, arXiv:1207.2159.

[37] B. Fuks, M. Klasen, D. R. Lamprea, and M. Rothering, "Precision predictions for electroweak superpartner production at hadron colliders with Resummino", *Eur. Phys. J. C* **73** (2013) 2480, doi:10.1140/epjc/s10052-013-2480-0, arXiv:1304.0790.

[38] NNPDF Collaboration, "Parton distributions for the LHC Run II", *JHEP* **04** (2015) 040, doi:10.1007/JHEP04(2015)040, arXiv:1410.8849.

[39] NNPDF Collaboration, "Parton distributions from high-precision collider data", *Eur. Phys. J. C* **77** (2017) 663, doi:10.1140/epjc/s10052-017-5199-5, arXiv:1706.00428.

[40] T. Sjöstrand et al., "An introduction to PYTHIA 8.2", *Comput. Phys. Commun.* **191** (2015) 159, doi:10.1016/j.cpc.2015.01.024, arXiv:1410.3012.

[41] CMS Collaboration, "Event generator tunes obtained from underlying event and multiparton scattering measurements", *Eur. Phys. J. C* **76** (2016) 155, doi:10.1140/epjc/s10052-016-3988-x, arXiv:1512.00815.

[42] CMS Collaboration, "Extraction and validation of a new set of CMS PYTHIA8 tunes from underlying-event measurements", (2019). arXiv:1903.12179. Submitted to *Eur. Phys. J. C*.

[43] R. Frederix and S. Frixione, "Merging meets matching in MC@NLO", *JHEP* **12** (2012) 061, doi:10.1007/JHEP12(2012)061, arXiv:1209.6215.

[44] GEANT4 Collaboration, "GEANT4—a simulation toolkit", *Nucl. Instrum. Meth. A* **506** (2003) 250, doi:10.1016/S0168-9002(03)01368-8.

[45] CMS Collaboration, "Particle-flow reconstruction and global event description with the CMS detector", *JINST* **12** (2017) P10003, doi:10.1088/1748-0221/12/10/P10003, arXiv:1706.04965.

[46] M. Cacciari, G. P. Salam, and G. Soyez, "The anti-k_{T} jet clustering algorithm", *JHEP* **04** (2008) 063, doi:10.1088/1126-6708/2008/04/063, arXiv:0802.1189.

[47] M. Cacciari, G. P. Salam, and G. Soyez, "FastJet user manual", *Eur. Phys. J. C* **72** (2012) 1896, doi:10.1140/epjc/s10052-012-1896-2, arXiv:1111.6097.

[48] M. Cacciari, G. P. Salam, and G. Soyez, "The catchment area of jets", *JHEP* **04** (2008) 005, doi:10.1088/1126-6708/2008/04/005, arXiv:0802.1188.

[49] M. Cacciari and G. P. Salam, "Pileup subtraction using jet areas", *Phys. Lett. B* **659** (2008) 119, doi:10.1016/j.physletb.2007.09.077, arXiv:0707.1378.

[50] CMS Collaboration, "Jet energy scale and resolution in the CMS experiment in pp collisions at 8 TeV", *JINST* **12** (2017) P02014, doi:10.1088/1748-0221/12/02/P02014, arXiv:1607.03663.

[51] CMS Collaboration, "Jet algorithms performance in 13 TeV data", CMS Physics Analysis Summary CMS-PAS-JME-16-003, 2017.

[52] CMS Collaboration, "Identification of heavy-flavour jets with the CMS detector in pp collisions at 13 TeV", *JINST* **13** (2018) P05011, doi:10.1088/1748-0221/13/05/P05011, arXiv:1712.07158.

[53] CMS Collaboration, "Performance of missing transverse momentum reconstruction in proton-proton collisions at $\sqrt{s} = 13$ TeV using the CMS detector", *JINST* **14** (2019) P07004, doi:10.1088/1748-0221/14/07/P07004, arXiv:1903.06078.

[54] CMS Collaboration, "Performance of electron reconstruction and selection with the CMS detector in proton-proton collisions at $\sqrt{s} = 8$ TeV", *JINST* **10** (2015) P06005, doi:10.1088/1748-0221/10/06/P06005, arXiv:1502.02701.

[55] CMS Collaboration, "Performance of the CMS muon detector and muon reconstruction with proton-proton collisions at $\sqrt{s} = 13$ TeV", *JINST* **13** (2018) P06015, doi:10.1088/1748-0221/13/06/P06015, arXiv:1804.04528.

[56] M. Cacciari et al., "The $t\bar{t}$ cross-section at 1.8 and 1.96 TeV: A study of the systematics due to parton densities and scale dependence", *JHEP* **04** (2004) 068, doi:10.1088/1126-6708/2004/04/068, arXiv:hep-ph/0303085.

[57] CMS Collaboration, "CMS luminosity measurements for the 2016 data-taking period", CMS Physics Analysis Summary CMS-PAS-LUM-17-001, 2017.

[58] CMS Collaboration, "CMS luminosity measurement for the 2017 data-taking period at $\sqrt{s} = 13$ TeV", CMS Physics Analysis Summary CMS-PAS-LUM-17-004, 2018.

[59] CMS Collaboration, "CMS luminosity measurement for the 2018 data-taking period at $\sqrt{s} = 13$ TeV", CMS Physics Analysis Summary CMS-PAS-LUM-18-002, 2019.

[60] CMS Collaboration, "Search for third-generation scalar leptoquarks in the tτ channel in proton-proton collisions at $\sqrt{s}$ = 8 TeV", *JHEP* **07** (2015) 042, doi:10.1007/JHEP07(2015)042, arXiv:1503.09049. [Erratum: doi:10.1007/JHEP11(2016)056].

[61] S. Baker and R. D. Cousins, "Clarification of the use of χ^2 and likelihood functions in fits to histograms", *Nucl. Instrum. Meth.* **221** (1984) 437, doi:10.1016/0167-5087(84)90016-4.

[62] E. Gross and O. Vitells, "Trial factors for the look elsewhere effect in high energy physics", *Eur. Phys. J. C* **70** (2010) 525, doi:10.1140/epjc/s10052-010-1470-8, arXiv:1005.1891.

[63] T. Junk, “Confidence level computation for combining searches with small statistics”, *Nucl. Instrum. Meth. A* **434** (1999) 435, doi:10.1016/S0168-9002(99)00498-2, arXiv:hep-ex/9902006.

[64] A. L. Read, “Presentation of search results: The CL_s technique”, *J. Phys. G* **28** (2002) 2693, doi:10.1088/0954-3899/28/10/313.

[65] G. Cowan, K. Cranmer, E. Gross, and O. Vitells, “Asymptotic formulae for likelihood-based tests of new physics”, *Eur. Phys. J. C* **71** (2011) 1554, doi:10.1140/epjc/s10052-011-1554-0, arXiv:1007.1727. [Erratum: doi:10.1140/epjc/s10052-013-2501-z].

[66] ATLAS and CMS Collaborations, “Procedure for the LHC Higgs boson search combination in summer 2011”, Technical Report CMS-NOTE-2011-005, ATL-PHYS-PUB-2011-11, 2011.

[67] LHC Higgs Cross Section Working Group, “Handbook of LHC Higgs cross sections: 4. deciphering the nature of the Higgs sector”, *CERN* (2016) doi:10.23731/CYRM-2017-002, arXiv:1610.07922.

A The CMS Collaboration

Yerevan Physics Institute, Yerevan, Armenia
A.M. Sirunyan[†], A. Tumasyan

Institut für Hochenergiephysik, Wien, Austria
W. Adam, F. Ambrogi, T. Bergauer, M. Dragicevic, J. Erö, A. Escalante Del Valle, M. Flechl, R. Frühwirth[1], M. Jeitler[1], N. Krammer, I. Krätschmer, D. Liko, T. Madlener, I. Mikulec, N. Rad, J. Schieck[1], R. Schöfbeck, M. Spanring, D. Spitzbart, W. Waltenberger, C.-E. Wulz[1], M. Zarucki

Institute for Nuclear Problems, Minsk, Belarus
V. Drugakov, V. Mossolov, J. Suarez Gonzalez

Universiteit Antwerpen, Antwerpen, Belgium
M.R. Darwish, E.A. De Wolf, D. Di Croce, X. Janssen, A. Lelek, M. Pieters, H. Rejeb Sfar, H. Van Haevermaet, P. Van Mechelen, S. Van Putte, N. Van Remortel

Vrije Universiteit Brussel, Brussel, Belgium
F. Blekman, E.S. Bols, S.S. Chhibra, J. D'Hondt, J. De Clercq, D. Lontkovskyi, S. Lowette, I. Marchesini, S. Moortgat, Q. Python, K. Skovpen, S. Tavernier, W. Van Doninck, P. Van Mulders

Université Libre de Bruxelles, Bruxelles, Belgium
D. Beghin, B. Bilin, B. Clerbaux, G. De Lentdecker, H. Delannoy, B. Dorney, L. Favart, A. Grebenyuk, A.K. Kalsi, A. Popov, N. Postiau, E. Starling, L. Thomas, C. Vander Velde, P. Vanlaer, D. Vannerom

Ghent University, Ghent, Belgium
T. Cornelis, D. Dobur, I. Khvastunov[2], M. Niedziela, C. Roskas, M. Tytgat, W. Verbeke, B. Vermassen, M. Vit

Université Catholique de Louvain, Louvain-la-Neuve, Belgium
O. Bondu, G. Bruno, C. Caputo, P. David, C. Delaere, M. Delcourt, A. Giammanco, V. Lemaitre, J. Prisciandaro, A. Saggio, M. Vidal Marono, P. Vischia, J. Zobec

Centro Brasileiro de Pesquisas Fisicas, Rio de Janeiro, Brazil
F.L. Alves, G.A. Alves, G. Correia Silva, C. Hensel, A. Moraes, P. Rebello Teles

Universidade do Estado do Rio de Janeiro, Rio de Janeiro, Brazil
E. Belchior Batista Das Chagas, W. Carvalho, J. Chinellato[3], E. Coelho, E.M. Da Costa, G.G. Da Silveira[4], D. De Jesus Damiao, C. De Oliveira Martins, S. Fonseca De Souza, L.M. Huertas Guativa, H. Malbouisson, J. Martins[5], D. Matos Figueiredo, M. Medina Jaime[6], M. Melo De Almeida, C. Mora Herrera, L. Mundim, H. Nogima, W.L. Prado Da Silva, L.J. Sanchez Rosas, A. Santoro, A. Sznajder, M. Thiel, E.J. Tonelli Manganote[3], F. Torres Da Silva De Araujo, A. Vilela Pereira

Universidade Estadual Paulista [a], Universidade Federal do ABC [b], São Paulo, Brazil
C.A. Bernardes[a], L. Calligaris[a], T.R. Fernandez Perez Tomei[a], E.M. Gregores[b], D.S. Lemos, P.G. Mercadante[b], S.F. Novaes[a], SandraS. Padula[a]

Institute for Nuclear Research and Nuclear Energy, Bulgarian Academy of Sciences, Sofia, Bulgaria
A. Aleksandrov, G. Antchev, R. Hadjiiska, P. Iaydjiev, M. Misheva, M. Rodozov, M. Shopova, G. Sultanov

University of Sofia, Sofia, Bulgaria
M. Bonchev, A. Dimitrov, T. Ivanov, L. Litov, B. Pavlov, P. Petkov

Beihang University, Beijing, China
W. Fang[7], X. Gao[7], L. Yuan

Institute of High Energy Physics, Beijing, China
G.M. Chen, H.S. Chen, M. Chen, C.H. Jiang, D. Leggat, H. Liao, Z. Liu, A. Spiezia, J. Tao, E. Yazgan, H. Zhang, S. Zhang[8], J. Zhao

State Key Laboratory of Nuclear Physics and Technology, Peking University, Beijing, China
A. Agapitos, Y. Ban, G. Chen, A. Levin, J. Li, L. Li, Q. Li, Y. Mao, S.J. Qian, D. Wang, Q. Wang

Tsinghua University, Beijing, China
M. Ahmad, Z. Hu, Y. Wang

Zhejiang University, Hangzhou, China
M. Xiao

Universidad de Los Andes, Bogota, Colombia
C. Avila, A. Cabrera, C. Florez, C.F. González Hernández, M.A. Segura Delgado

Universidad de Antioquia, Medellin, Colombia
J. Mejia Guisao, J.D. Ruiz Alvarez, C.A. Salazar González, N. Vanegas Arbelaez

University of Split, Faculty of Electrical Engineering, Mechanical Engineering and Naval Architecture, Split, Croatia
D. Giljanović, N. Godinovic, D. Lelas, I. Puljak, T. Sculac

University of Split, Faculty of Science, Split, Croatia
Z. Antunovic, M. Kovac

Institute Rudjer Boskovic, Zagreb, Croatia
V. Brigljevic, D. Ferencek, K. Kadija, B. Mesic, M. Roguljic, A. Starodumov[9], T. Susa

University of Cyprus, Nicosia, Cyprus
M.W. Ather, A. Attikis, E. Erodotou, A. Ioannou, M. Kolosova, S. Konstantinou, G. Mavromanolakis, J. Mousa, C. Nicolaou, F. Ptochos, P.A. Razis, H. Rykaczewski, D. Tsiakkouri

Charles University, Prague, Czech Republic
M. Finger[10], M. Finger Jr.[10], A. Kveton, J. Tomsa

Escuela Politecnica Nacional, Quito, Ecuador
E. Ayala

Universidad San Francisco de Quito, Quito, Ecuador
E. Carrera Jarrin

Academy of Scientific Research and Technology of the Arab Republic of Egypt, Egyptian Network of High Energy Physics, Cairo, Egypt
Y. Assran[11,12], S. Elgammal[12]

National Institute of Chemical Physics and Biophysics, Tallinn, Estonia
S. Bhowmik, A. Carvalho Antunes De Oliveira, R.K. Dewanjee, K. Ehataht, M. Kadastik, M. Raidal, C. Veelken

Department of Physics, University of Helsinki, Helsinki, Finland
P. Eerola, L. Forthomme, H. Kirschenmann, K. Osterberg, M. Voutilainen

Helsinki Institute of Physics, Helsinki, Finland
F. Garcia, J. Havukainen, J.K. Heikkilä, V. Karimäki, M.S. Kim, R. Kinnunen, T. Lampén, K. Lassila-Perini, S. Laurila, S. Lehti, T. Lindén, P. Luukka, T. Mäenpää, H. Siikonen, E. Tuominen, J. Tuominiemi

Lappeenranta University of Technology, Lappeenranta, Finland
T. Tuuva

IRFU, CEA, Université Paris-Saclay, Gif-sur-Yvette, France
M. Besancon, F. Couderc, M. Dejardin, D. Denegri, B. Fabbro, J.L. Faure, F. Ferri, S. Ganjour, A. Givernaud, P. Gras, G. Hamel de Monchenault, P. Jarry, C. Leloup, B. Lenzi, E. Locci, J. Malcles, J. Rander, A. Rosowsky, M.Ö. Sahin, A. Savoy-Navarro[13], M. Titov, G.B. Yu

Laboratoire Leprince-Ringuet, CNRS/IN2P3, Ecole Polytechnique, Institut Polytechnique de Paris
S. Ahuja, C. Amendola, F. Beaudette, P. Busson, C. Charlot, B. Diab, G. Falmagne, R. Granier de Cassagnac, I. Kucher, A. Lobanov, C. Martin Perez, M. Nguyen, C. Ochando, P. Paganini, J. Rembser, R. Salerno, J.B. Sauvan, Y. Sirois, A. Zabi, A. Zghiche

Université de Strasbourg, CNRS, IPHC UMR 7178, Strasbourg, France
J.-L. Agram[14], J. Andrea, D. Bloch, G. Bourgatte, J.-M. Brom, E.C. Chabert, C. Collard, E. Conte[14], J.-C. Fontaine[14], D. Gelé, U. Goerlach, M. Jansová, A.-C. Le Bihan, N. Tonon, P. Van Hove

Centre de Calcul de l'Institut National de Physique Nucleaire et de Physique des Particules, CNRS/IN2P3, Villeurbanne, France
S. Gadrat

Université de Lyon, Université Claude Bernard Lyon 1, CNRS-IN2P3, Institut de Physique Nucléaire de Lyon, Villeurbanne, France
S. Beauceron, C. Bernet, G. Boudoul, C. Camen, A. Carle, N. Chanon, R. Chierici, D. Contardo, P. Depasse, H. El Mamouni, J. Fay, S. Gascon, M. Gouzevitch, B. Ille, Sa. Jain, F. Lagarde, I.B. Laktineh, H. Lattaud, A. Lesauvage, M. Lethuillier, L. Mirabito, S. Perries, V. Sordini, L. Torterotot, G. Touquet, M. Vander Donckt, S. Viret

Georgian Technical University, Tbilisi, Georgia
T. Toriashvili[15]

Tbilisi State University, Tbilisi, Georgia
Z. Tsamalaidze[10]

RWTH Aachen University, I. Physikalisches Institut, Aachen, Germany
C. Autermann, L. Feld, K. Klein, M. Lipinski, D. Meuser, A. Pauls, M. Preuten, M.P. Rauch, J. Schulz, M. Teroerde, B. Wittmer

RWTH Aachen University, III. Physikalisches Institut A, Aachen, Germany
M. Erdmann, B. Fischer, S. Ghosh, T. Hebbeker, K. Hoepfner, H. Keller, L. Mastrolorenzo, M. Merschmeyer, A. Meyer, P. Millet, G. Mocellin, S. Mondal, S. Mukherjee, D. Noll, A. Novak, T. Pook, A. Pozdnyakov, T. Quast, M. Radziej, Y. Rath, H. Reithler, J. Roemer, A. Schmidt, S.C. Schuler, A. Sharma, S. Wiedenbeck, S. Zaleski

RWTH Aachen University, III. Physikalisches Institut B, Aachen, Germany
G. Flügge, W. Haj Ahmad[16], O. Hlushchenko, T. Kress, T. Müller, A. Nowack, C. Pistone, O. Pooth, D. Roy, H. Sert, A. Stahl[17]

Deutsches Elektronen-Synchrotron, Hamburg, Germany
M. Aldaya Martin, P. Asmuss, I. Babounikau, H. Bakhshiansohi, K. Beernaert, O. Behnke, A. Bermúdez Martínez, D. Bertsche, A.A. Bin Anuar, K. Borras[18], V. Botta, A. Campbell, A. Cardini, P. Connor, S. Consuegra Rodríguez, C. Contreras-Campana, V. Danilov, A. De Wit, M.M. Defranchis, C. Diez Pardos, D. Domínguez Damiani, G. Eckerlin, D. Eckstein, T. Eichhorn, A. Elwood, E. Eren, E. Gallo[19], A. Geiser, A. Grohsjean, M. Guthoff, M. Haranko, A. Harb, A. Jafari, N.Z. Jomhari, H. Jung, A. Kasem[18], M. Kasemann, H. Kaveh, J. Keaveney, C. Kleinwort, J. Knolle, D. Krücker, W. Lange, T. Lenz, J. Lidrych, K. Lipka, W. Lohmann[20], R. Mankel, I.-A. Melzer-Pellmann, A.B. Meyer, M. Meyer, M. Missiroli, J. Mnich, A. Mussgiller, V. Myronenko, D. Pérez Adán, S.K. Pflitsch, D. Pitzl, A. Raspereza, A. Saibel, M. Savitskyi, V. Scheurer, P. Schütze, C. Schwanenberger, R. Shevchenko, A. Singh, H. Tholen, O. Turkot, A. Vagnerini, M. Van De Klundert, R. Walsh, Y. Wen, K. Wichmann, C. Wissing, O. Zenaiev, R. Zlebcik

University of Hamburg, Hamburg, Germany
R. Aggleton, S. Bein, L. Benato, A. Benecke, V. Blobel, T. Dreyer, A. Ebrahimi, F. Feindt, A. Fröhlich, C. Garbers, E. Garutti, D. Gonzalez, P. Gunnellini, J. Haller, A. Hinzmann, A. Karavdina, G. Kasieczka, R. Klanner, R. Kogler, N. Kovalchuk, S. Kurz, V. Kutzner, J. Lange, T. Lange, A. Malara, J. Multhaup, C.E.N. Niemeyer, A. Perieanu, A. Reimers, O. Rieger, C. Scharf, P. Schleper, S. Schumann, J. Schwandt, J. Sonneveld, H. Stadie, G. Steinbrück, F.M. Stober, B. Vormwald, I. Zoi

Karlsruher Institut fuer Technologie, Karlsruhe, Germany
M. Akbiyik, C. Barth, M. Baselga, S. Baur, T. Berger, E. Butz, R. Caspart, T. Chwalek, W. De Boer, A. Dierlamm, K. El Morabit, N. Faltermann, M. Giffels, P. Goldenzweig, A. Gottmann, M.A. Harrendorf, F. Hartmann[17], U. Husemann, S. Kudella, S. Mitra, M.U. Mozer, D. Müller, Th. Müller, M. Musich, A. Nürnberg, G. Quast, K. Rabbertz, M. Schröder, I. Shvetsov, H.J. Simonis, R. Ulrich, M. Wassmer, M. Weber, C. Wöhrmann, R. Wolf

Institute of Nuclear and Particle Physics (INPP), NCSR Demokritos, Aghia Paraskevi, Greece
G. Anagnostou, P. Asenov, G. Daskalakis, T. Geralis, A. Kyriakis, D. Loukas, G. Paspalaki

National and Kapodistrian University of Athens, Athens, Greece
M. Diamantopoulou, G. Karathanasis, P. Kontaxakis, A. Manousakis-katsikakis, A. Panagiotou, I. Papavergou, N. Saoulidou, A. Stakia, K. Theofilatos, K. Vellidis, E. Vourliotis

National Technical University of Athens, Athens, Greece
G. Bakas, K. Kousouris, I. Papakrivopoulos, G. Tsipolitis

University of Ioánnina, Ioánnina, Greece
I. Evangelou, C. Foudas, P. Gianneios, P. Katsoulis, P. Kokkas, S. Mallios, K. Manitara, N. Manthos, I. Papadopoulos, J. Strologas, F.A. Triantis, D. Tsitsonis

MTA-ELTE Lendület CMS Particle and Nuclear Physics Group, Eötvös Loránd University, Budapest, Hungary
M. Bartók[21], R. Chudasama, M. Csanad, P. Major, K. Mandal, A. Mehta, M.I. Nagy, G. Pasztor, O. Surányi, G.I. Veres

Wigner Research Centre for Physics, Budapest, Hungary
G. Bencze, C. Hajdu, D. Horvath[22], F. Sikler, T.. Vámi, V. Veszpremi, G. Vesztergombi[†]

Institute of Nuclear Research ATOMKI, Debrecen, Hungary
N. Beni, S. Czellar, J. Karancsi[21], J. Molnar, Z. Szillasi

Institute of Physics, University of Debrecen, Debrecen, Hungary
P. Raics, D. Teyssier, Z.L. Trocsanyi, B. Ujvari

Eszterhazy Karoly University, Karoly Robert Campus, Gyongyos, Hungary
T. Csorgo, W.J. Metzger, F. Nemes, T. Novak

Indian Institute of Science (IISc), Bangalore, India
S. Choudhury, J.R. Komaragiri, P.C. Tiwari

National Institute of Science Education and Research, HBNI, Bhubaneswar, India
S. Bahinipati[24], C. Kar, G. Kole, P. Mal, V.K. Muraleedharan Nair Bindhu, A. Nayak[25], D.K. Sahoo[24], S.K. Swain

Panjab University, Chandigarh, India
S. Bansal, S.B. Beri, V. Bhatnagar, S. Chauhan, R. Chawla, N. Dhingra, R. Gupta, A. Kaur, M. Kaur, S. Kaur, P. Kumari, M. Lohan, M. Meena, K. Sandeep, S. Sharma, J.B. Singh, A.K. Virdi, G. Walia

University of Delhi, Delhi, India
A. Bhardwaj, B.C. Choudhary, R.B. Garg, M. Gola, S. Keshri, Ashok Kumar, M. Naimuddin, P. Priyanka, K. Ranjan, Aashaq Shah, R. Sharma

Saha Institute of Nuclear Physics, HBNI, Kolkata, India
R. Bhardwaj[26], M. Bharti[26], R. Bhattacharya, S. Bhattacharya, U. Bhawandeep[26], D. Bhowmik, S. Dutta, S. Ghosh, B. Gomber[27], M. Maity[28], K. Mondal, S. Nandan, A. Purohit, P.K. Rout, G. Saha, S. Sarkar, T. Sarkar[28], M. Sharan, B. Singh[26], S. Thakur[26]

Indian Institute of Technology Madras, Madras, India
P.K. Behera, P. Kalbhor, A. Muhammad, P.R. Pujahari, A. Sharma, A.K. Sikdar

Bhabha Atomic Research Centre, Mumbai, India
D. Dutta, V. Jha, V. Kumar, D.K. Mishra, P.K. Netrakanti, L.M. Pant, P. Shukla

Tata Institute of Fundamental Research-A, Mumbai, India
T. Aziz, M.A. Bhat, S. Dugad, G.B. Mohanty, N. Sur, RavindraKumar Verma

Tata Institute of Fundamental Research-B, Mumbai, India
S. Banerjee, S. Bhattacharya, S. Chatterjee, P. Das, M. Guchait, S. Karmakar, S. Kumar, G. Majumder, K. Mazumdar, N. Sahoo, S. Sawant

Indian Institute of Science Education and Research (IISER), Pune, India
S. Dube, B. Kansal, A. Kapoor, K. Kothekar, S. Pandey, A. Rane, A. Rastogi, S. Sharma

Institute for Research in Fundamental Sciences (IPM), Tehran, Iran
S. Chenarani[29], E. Eskandari Tadavani, S.M. Etesami[29], M. Khakzad, M. Mohammadi Najafabadi, M. Naseri, F. Rezaei Hosseinabadi

University College Dublin, Dublin, Ireland
M. Felcini, M. Grunewald

INFN Sezione di Bari [a], Università di Bari [b], Politecnico di Bari [c], Bari, Italy
M. Abbrescia[a,b], R. Aly[a,b,30], C. Calabria[a,b], A. Colaleo[a], D. Creanza[a,c], L. Cristella[a,b], N. De Filippis[a,c], M. De Palma[a,b], A. Di Florio[a,b], W. Elmetenawee[a,b], L. Fiore[a], A. Gelmi[a,b], G. Iaselli[a,c], M. Ince[a,b], S. Lezki[a,b], G. Maggi[a,c], M. Maggi[a], J.A. Merlin, G. Miniello[a,b], S. My[a,b], S. Nuzzo[a,b], A. Pompili[a,b], G. Pugliese[a,c], R. Radogna[a], A. Ranieri[a], G. Selvaggi[a,b], L. Silvestris[a], F.M. Simone[a,b], R. Venditti[a], P. Verwilligen[a]

INFN Sezione di Bologna [a], Università di Bologna [b], Bologna, Italy
G. Abbiendi[a], C. Battilana[a,b], D. Bonacorsi[a,b], L. Borgonovi[a,b], S. Braibant-Giacomelli[a,b], R. Campanini[a,b], P. Capiluppi[a,b], A. Castro[a,b], F.R. Cavallo[a], C. Ciocca[a], G. Codispoti[a,b], M. Cuffiani[a,b], G.M. Dallavalle[a], F. Fabbri[a], A. Fanfani[a,b], E. Fontanesi[a,b], P. Giacomelli[a], C. Grandi[a], L. Guiducci[a,b], F. Iemmi[a,b], S. Lo Meo[a,31], S. Marcellini[a], G. Masetti[a], F.L. Navarria[a,b], A. Perrotta[a], F. Primavera[a,b], A.M. Rossi[a,b], T. Rovelli[a,b], G.P. Siroli[a,b], N. Tosi[a]

INFN Sezione di Catania [a], Università di Catania [b], Catania, Italy
S. Albergo[a,b,32], S. Costa[a,b], A. Di Mattia[a], R. Potenza[a,b], A. Tricomi[a,b,32], C. Tuve[a,b]

INFN Sezione di Firenze [a], Università di Firenze [b], Firenze, Italy
G. Barbagli[a], A. Cassese, R. Ceccarelli, V. Ciulli[a,b], C. Civinini[a], R. D'Alessandro[a,b], F. Fiori[a,c], E. Focardi[a,b], G. Latino[a,b], P. Lenzi[a,b], M. Meschini[a], S. Paoletti[a], G. Sguazzoni[a], L. Viliani[a]

INFN Laboratori Nazionali di Frascati, Frascati, Italy
L. Benussi, S. Bianco, D. Piccolo

INFN Sezione di Genova [a], Università di Genova [b], Genova, Italy
M. Bozzo[a,b], F. Ferro[a], R. Mulargia[a,b], E. Robutti[a], S. Tosi[a,b]

INFN Sezione di Milano-Bicocca [a], Università di Milano-Bicocca [b], Milano, Italy
A. Benaglia[a], A. Beschi[a,b], F. Brivio[a,b], V. Ciriolo[a,b,17], M.E. Dinardo[a,b], P. Dini[a], S. Gennai[a], A. Ghezzi[a,b], P. Govoni[a,b], L. Guzzi[a,b], M. Malberti[a], S. Malvezzi[a], D. Menasce[a], F. Monti[a,b], L. Moroni[a], M. Paganoni[a,b], D. Pedrini[a], S. Ragazzi[a,b], T. Tabarelli de Fatis[a,b], D. Valsecchi[a,b], D. Zuolo[a,b]

INFN Sezione di Napoli [a], Università di Napoli 'Federico II' [b], Napoli, Italy, Università della Basilicata [c], Potenza, Italy, Università G. Marconi [d], Roma, Italy
S. Buontempo[a], N. Cavallo[a,c], A. De Iorio[a,b], A. Di Crescenzo[a,b], F. Fabozzi[a,c], F. Fienga[a], G. Galati[a], A.O.M. Iorio[a,b], L. Lista[a,b], S. Meola[a,d,17], P. Paolucci[a,17], B. Rossi[a], C. Sciacca[a,b], E. Voevodina[a,b]

INFN Sezione di Padova [a], Università di Padova [b], Padova, Italy, Università di Trento [c], Trento, Italy
P. Azzi[a], N. Bacchetta[a], D. Bisello[a,b], A. Boletti[a,b], A. Bragagnolo[a,b], R. Carlin[a,b], P. Checchia[a], P. De Castro Manzano[a], T. Dorigo[a], U. Dosselli[a], F. Gasparini[a,b], U. Gasparini[a,b], A. Gozzelino[a], S.Y. Hoh[a,b], P. Lujan[a], M. Margoni[a,b], A.T. Meneguzzo[a,b], J. Pazzini[a,b], M. Presilla[b], P. Ronchese[a,b], R. Rossin[a,b], F. Simonetto[a,b], A. Tiko[a], M. Tosi[a,b], M. Zanetti[a,b], P. Zotto[a,b], G. Zumerle[a,b]

INFN Sezione di Pavia [a], Università di Pavia [b], Pavia, Italy
A. Braghieri[a], D. Fiorina[a,b], P. Montagna[a,b], S.P. Ratti[a,b], V. Re[a], M. Ressegotti[a,b], C. Riccardi[a,b], P. Salvini[a], I. Vai[a], P. Vitulo[a,b]

INFN Sezione di Perugia [a], Università di Perugia [b], Perugia, Italy
M. Biasini[a,b], G.M. Bilei[a], D. Ciangottini[a,b], L. Fanò[a,b], P. Lariccia[a,b], R. Leonardi[a,b], E. Manoni[a], G. Mantovani[a,b], V. Mariani[a,b], M. Menichelli[a], A. Rossi[a,b], A. Santocchia[a,b], D. Spiga[a]

INFN Sezione di Pisa [a], Università di Pisa [b], Scuola Normale Superiore di Pisa [c], Pisa, Italy
K. Androsov[a], P. Azzurri[a], G. Bagliesi[a], V. Bertacchi[a,c], L. Bianchini[a], T. Boccali[a], R. Castaldi[a], M.A. Ciocci[a,b], R. Dell'Orso[a], S. Donato[a], G. Fedi[a], L. Giannini[a,c], A. Giassi[a], M.T. Grippo[a], F. Ligabue[a,c], E. Manca[a,c], G. Mandorli[a,c], A. Messineo[a,b], F. Palla[a], A. Rizzi[a,b], G. Rolandi[33], S. Roy Chowdhury, A. Scribano[a], P. Spagnolo[a], R. Tenchini[a], G. Tonelli[a,b], N. Turini, A. Venturi[a], P.G. Verdini[a]

INFN Sezione di Roma [a], Sapienza Università di Roma [b], Rome, Italy
F. Cavallari[a], M. Cipriani[a,b], D. Del Re[a,b], E. Di Marco[a], M. Diemoz[a], E. Longo[a,b], P. Meridiani[a], G. Organtini[a,b], F. Pandolfi[a], R. Paramatti[a,b], C. Quaranta[a,b], S. Rahatlou[a,b], C. Rovelli[a], F. Santanastasio[a,b], L. Soffi[a,b]

INFN Sezione di Torino [a], Università di Torino [b], Torino, Italy, Università del Piemonte Orientale [c], Novara, Italy
N. Amapane[a,b], R. Arcidiacono[a,c], S. Argiro[a,b], M. Arneodo[a,c], N. Bartosik[a], R. Bellan[a,b], A. Bellora, C. Biino[a], A. Cappati[a,b], N. Cartiglia[a], S. Cometti[a], M. Costa[a,b], R. Covarelli[a,b], N. Demaria[a], B. Kiani[a,b], F. Legger, C. Mariotti[a], S. Maselli[a], E. Migliore[a,b], V. Monaco[a,b], E. Monteil[a,b], M. Monteno[a], M.M. Obertino[a,b], G. Ortona[a,b], L. Pacher[a,b], N. Pastrone[a], M. Pelliccioni[a], G.L. Pinna Angioni[a,b], A. Romero[a,b], M. Ruspa[a,c], R. Salvatico[a,b], V. Sola[a], A. Solano[a,b], D. Soldi[a,b], A. Staiano[a], D. Trocino[a,b]

INFN Sezione di Trieste [a], Università di Trieste [b], Trieste, Italy
S. Belforte[a], V. Candelise[a,b], M. Casarsa[a], F. Cossutti[a], A. Da Rold[a,b], G. Della Ricca[a,b], F. Vazzoler[a,b], A. Zanetti[a]

Kyungpook National University, Daegu, Korea
B. Kim, D.H. Kim, G.N. Kim, J. Lee, S.W. Lee, C.S. Moon, Y.D. Oh, S.I. Pak, S. Sekmen, D.C. Son, Y.C. Yang

Chonnam National University, Institute for Universe and Elementary Particles, Kwangju, Korea
H. Kim, D.H. Moon, G. Oh

Hanyang University, Seoul, Korea
B. Francois, T.J. Kim, J. Park

Korea University, Seoul, Korea
S. Cho, S. Choi, Y. Go, S. Ha, B. Hong, K. Lee, K.S. Lee, J. Lim, J. Park, S.K. Park, Y. Roh, J. Yoo

Kyung Hee University, Department of Physics
J. Goh

Sejong University, Seoul, Korea
H.S. Kim

Seoul National University, Seoul, Korea
J. Almond, J.H. Bhyun, J. Choi, S. Jeon, J. Kim, J.S. Kim, H. Lee, K. Lee, S. Lee, K. Nam, M. Oh, S.B. Oh, B.C. Radburn-Smith, U.K. Yang, H.D. Yoo, I. Yoon

University of Seoul, Seoul, Korea
D. Jeon, J.H. Kim, J.S.H. Lee, I.C. Park, I.J Watson

Sungkyunkwan University, Suwon, Korea
Y. Choi, C. Hwang, Y. Jeong, J. Lee, Y. Lee, I. Yu

Riga Technical University, Riga, Latvia
V. Veckalns[34]

Vilnius University, Vilnius, Lithuania
V. Dudenas, A. Juodagalvis, A. Rinkevicius, G. Tamulaitis, J. Vaitkus

National Centre for Particle Physics, Universiti Malaya, Kuala Lumpur, Malaysia
Z.A. Ibrahim, F. Mohamad Idris[35], W.A.T. Wan Abdullah, M.N. Yusli, Z. Zolkapli

Universidad de Sonora (UNISON), Hermosillo, Mexico
J.F. Benitez, A. Castaneda Hernandez, J.A. Murillo Quijada, L. Valencia Palomo

Centro de Investigacion y de Estudios Avanzados del IPN, Mexico City, Mexico
H. Castilla-Valdez, E. De La Cruz-Burelo, I. Heredia-De La Cruz[36], R. Lopez-Fernandez, A. Sanchez-Hernandez

Universidad Iberoamericana, Mexico City, Mexico
S. Carrillo Moreno, C. Oropeza Barrera, M. Ramirez-Garcia, F. Vazquez Valencia

Benemerita Universidad Autonoma de Puebla, Puebla, Mexico
J. Eysermans, I. Pedraza, H.A. Salazar Ibarguen, C. Uribe Estrada

Universidad Autónoma de San Luis Potosí, San Luis Potosí, Mexico
A. Morelos Pineda

University of Montenegro, Podgorica, Montenegro
J. Mijuskovic[2], N. Raicevic

University of Auckland, Auckland, New Zealand
D. Krofcheck

University of Canterbury, Christchurch, New Zealand
S. Bheesette, P.H. Butler

National Centre for Physics, Quaid-I-Azam University, Islamabad, Pakistan
A. Ahmad, M. Ahmad, Q. Hassan, H.R. Hoorani, W.A. Khan, M.A. Shah, M. Shoaib, M. Waqas

AGH University of Science and Technology Faculty of Computer Science, Electronics and Telecommunications, Krakow, Poland
V. Avati, L. Grzanka, M. Malawski

National Centre for Nuclear Research, Swierk, Poland
H. Bialkowska, M. Bluj, B. Boimska, M. Górski, M. Kazana, M. Szleper, P. Zalewski

Institute of Experimental Physics, Faculty of Physics, University of Warsaw, Warsaw, Poland
K. Bunkowski, A. Byszuk[37], K. Doroba, A. Kalinowski, M. Konecki, J. Krolikowski, M. Olszewski, M. Walczak

Laboratório de Instrumentação e Física Experimental de Partículas, Lisboa, Portugal
M. Araujo, P. Bargassa, D. Bastos, A. Di Francesco, P. Faccioli, B. Galinhas, M. Gallinaro, J. Hollar, N. Leonardo, T. Niknejad, J. Seixas, K. Shchelina, G. Strong, O. Toldaiev, J. Varela

Joint Institute for Nuclear Research, Dubna, Russia
S. Afanasiev, P. Bunin, M. Gavrilenko, I. Golutvin, I. Gorbunov, A. Kamenev, V. Karjavine, A. Lanev, A. Malakhov, V. Matveev[38,39], P. Moisenz, V. Palichik, V. Perelygin, M. Savina, S. Shmatov, S. Shulha, N. Skatchkov, V. Smirnov, N. Voytishin, A. Zarubin

Petersburg Nuclear Physics Institute, Gatchina (St. Petersburg), Russia
L. Chtchipounov, V. Golovtcov, Y. Ivanov, V. Kim[40], E. Kuznetsova[41], P. Levchenko, V. Murzin, V. Oreshkin, I. Smirnov, D. Sosnov, V. Sulimov, L. Uvarov, A. Vorobyev

Institute for Nuclear Research, Moscow, Russia
Yu. Andreev, A. Dermenev, S. Gninenko, N. Golubev, A. Karneyeu, M. Kirsanov, N. Krasnikov, A. Pashenkov, D. Tlisov, A. Toropin

Institute for Theoretical and Experimental Physics named by A.I. Alikhanov of NRC 'Kurchatov Institute', Moscow, Russia
V. Epshteyn, V. Gavrilov, N. Lychkovskaya, A. Nikitenko[42], V. Popov, I. Pozdnyakov, G. Safronov, A. Spiridonov, A. Stepennov, M. Toms, E. Vlasov, A. Zhokin

Moscow Institute of Physics and Technology, Moscow, Russia
T. Aushev

National Research Nuclear University 'Moscow Engineering Physics Institute' (MEPhI), Moscow, Russia
O. Bychkova, R. Chistov[43], M. Danilov[43], S. Polikarpov[43], E. Tarkovskii

P.N. Lebedev Physical Institute, Moscow, Russia
V. Andreev, M. Azarkin, I. Dremin, M. Kirakosyan, A. Terkulov

Skobeltsyn Institute of Nuclear Physics, Lomonosov Moscow State University, Moscow, Russia
A. Baskakov, A. Belyaev, E. Boos, V. Bunichev, M. Dubinin[44], L. Dudko, A. Ershov, A. Gribushin, V. Klyukhin, O. Kodolova, I. Lokhtin, S. Obraztsov, V. Savrin

Novosibirsk State University (NSU), Novosibirsk, Russia
A. Barnyakov[45], V. Blinov[45], T. Dimova[45], L. Kardapoltsev[45], Y. Skovpen[45]

Institute for High Energy Physics of National Research Centre 'Kurchatov Institute', Protvino, Russia
I. Azhgirey, I. Bayshev, S. Bitioukov, V. Kachanov, D. Konstantinov, P. Mandrik, V. Petrov, R. Ryutin, S. Slabospitskii, A. Sobol, S. Troshin, N. Tyurin, A. Uzunian, A. Volkov

National Research Tomsk Polytechnic University, Tomsk, Russia
A. Babaev, A. Iuzhakov, V. Okhotnikov

Tomsk State University, Tomsk, Russia
V. Borchsh, V. Ivanchenko, E. Tcherniaev

University of Belgrade: Faculty of Physics and VINCA Institute of Nuclear Sciences
P. Adzic[46], P. Cirkovic, M. Dordevic, P. Milenovic, J. Milosevic, M. Stojanovic

Centro de Investigaciones Energéticas Medioambientales y Tecnológicas (CIEMAT), Madrid, Spain
M. Aguilar-Benitez, J. Alcaraz Maestre, A. lvarez Fernández, I. Bachiller, M. Barrio Luna, CristinaF. Bedoya, J.A. Brochero Cifuentes, C.A. Carrillo Montoya, M. Cepeda, M. Cerrada, N. Colino, B. De La Cruz, A. Delgado Peris, J.P. Fernández Ramos, J. Flix, M.C. Fouz, O. Gonzalez Lopez, S. Goy Lopez, J.M. Hernandez, M.I. Josa, D. Moran, . Navarro Tobar, A. Pérez-Calero Yzquierdo, J. Puerta Pelayo, I. Redondo, L. Romero, S. Sánchez Navas, M.S. Soares, A. Triossi, C. Willmott

Universidad Autónoma de Madrid, Madrid, Spain
C. Albajar, J.F. de Trocóniz, R. Reyes-Almanza

Universidad de Oviedo, Instituto Universitario de Ciencias y Tecnologías Espaciales de Asturias (ICTEA), Oviedo, Spain
B. Alvarez Gonzalez, J. Cuevas, C. Erice, J. Fernandez Menendez, S. Folgueras, I. Gonzalez Caballero, J.R. González Fernández, E. Palencia Cortezon, V. Rodríguez Bouza, S. Sanchez Cruz

Instituto de Física de Cantabria (IFCA), CSIC-Universidad de Cantabria, Santander, Spain
I.J. Cabrillo, A. Calderon, B. Chazin Quero, J. Duarte Campderros, M. Fernandez,

P.J. Fernández Manteca, A. García Alonso, G. Gomez, C. Martinez Rivero, P. Martinez Ruiz del Arbol, F. Matorras, J. Piedra Gomez, C. Prieels, T. Rodrigo, A. Ruiz-Jimeno, L. Russo[47], L. Scodellaro, I. Vila, J.M. Vizan Garcia

University of Colombo, Colombo, Sri Lanka
K. Malagalage

University of Ruhuna, Department of Physics, Matara, Sri Lanka
W.G.D. Dharmaratna, N. Wickramage

CERN, European Organization for Nuclear Research, Geneva, Switzerland
D. Abbaneo, B. Akgun, E. Auffray, G. Auzinger, J. Baechler, P. Baillon, A.H. Ball, D. Barney, J. Bendavid, M. Bianco, A. Bocci, P. Bortignon, E. Bossini, C. Botta, E. Brondolin, T. Camporesi, A. Caratelli, G. Cerminara, E. Chapon, G. Cucciati, D. d'Enterria, A. Dabrowski, N. Daci, V. Daponte, A. David, O. Davignon, A. De Roeck, M. Deile, M. Dobson, M. Dünser, N. Dupont, A. Elliott-Peisert, N. Emriskova, F. Fallavollita[48], D. Fasanella, S. Fiorendi, G. Franzoni, J. Fulcher, W. Funk, S. Giani, D. Gigi, K. Gill, F. Glege, L. Gouskos, M. Gruchala, M. Guilbaud, D. Gulhan, J. Hegeman, C. Heidegger, Y. Iiyama, V. Innocente, T. James, P. Janot, O. Karacheban[20], J. Kaspar, J. Kieseler, M. Krammer[1], N. Kratochwil, C. Lange, P. Lecoq, C. Lourenço, L. Malgeri, M. Mannelli, A. Massironi, F. Meijers, S. Mersi, E. Meschi, F. Moortgat, M. Mulders, J. Ngadiuba, J. Niedziela, S. Nourbakhsh, S. Orfanelli, L. Orsini, F. Pantaleo[17], L. Pape, E. Perez, M. Peruzzi, A. Petrilli, G. Petrucciani, A. Pfeiffer, M. Pierini, F.M. Pitters, D. Rabady, A. Racz, M. Rieger, M. Rovere, H. Sakulin, J. Salfeld-Nebgen, C. Schäfer, C. Schwick, M. Selvaggi, A. Sharma, P. Silva, W. Snoeys, P. Sphicas[49], J. Steggemann, S. Summers, V.R. Tavolaro, D. Treille, A. Tsirou, G.P. Van Onsem, A. Vartak, M. Verzetti, W.D. Zeuner

Paul Scherrer Institut, Villigen, Switzerland
L. Caminada[50], K. Deiters, W. Erdmann, R. Horisberger, Q. Ingram, H.C. Kaestli, D. Kotlinski, U. Langenegger, T. Rohe, S.A. Wiederkehr

ETH Zurich - Institute for Particle Physics and Astrophysics (IPA), Zurich, Switzerland
M. Backhaus, P. Berger, N. Chernyavskaya, G. Dissertori, M. Dittmar, M. Donegà, C. Dorfer, T.A. Gómez Espinosa, C. Grab, D. Hits, W. Lustermann, R.A. Manzoni, M.T. Meinhard, F. Micheli, P. Musella, F. Nessi-Tedaldi, F. Pauss, G. Perrin, L. Perrozzi, S. Pigazzini, M.G. Ratti, M. Reichmann, C. Reissel, T. Reitenspiess, B. Ristic, D. Ruini, D.A. Sanz Becerra, M. Schönenberger, L. Shchutska, M.L. Vesterbacka Olsson, R. Wallny, D.H. Zhu

Universität Zürich, Zurich, Switzerland
T.K. Aarrestad, C. Amsler[51], D. Brzhechko, M.F. Canelli, A. De Cosa, R. Del Burgo, B. Kilminster, S. Leontsinis, V.M. Mikuni, I. Neutelings, G. Rauco, P. Robmann, K. Schweiger, C. Seitz, Y. Takahashi, S. Wertz, A. Zucchetta

National Central University, Chung-Li, Taiwan
T.H. Doan, C.M. Kuo, W. Lin, A. Roy, S.S. Yu

National Taiwan University (NTU), Taipei, Taiwan
P. Chang, Y. Chao, K.F. Chen, P.H. Chen, W.-S. Hou, Y.y. Li, R.-S. Lu, E. Paganis, A. Psallidas, A. Steen

Chulalongkorn University, Faculty of Science, Department of Physics, Bangkok, Thailand
B. Asavapibhop, C. Asawatangtrakuldee, N. Srimanobhas, N. Suwonjandee

ukurova University, Physics Department, Science and Art Faculty, Adana, Turkey
A. Bat, F. Boran, A. Celik[52], S. Cerci[53], S. Damarseckin[54], Z.S. Demiroglu, F. Dolek, C. Dozen[55],

I. Dumanoglu, G. Gokbulut, EmineGurpinar Guler[56], Y. Guler, I. Hos[57], C. Isik, E.E. Kangal[58], O. Kara, A. Kayis Topaksu, U. Kiminsu, G. Onengut, K. Ozdemir[59], S. Ozturk[60], A.E. Simsek, D. Sunar Cerci[53], U.G. Tok, S. Turkcapar, I.S. Zorbakir, C. Zorbilmez

Middle East Technical University, Physics Department, Ankara, Turkey
B. Isildak[61], G. Karapinar[62], M. Yalvac

Bogazici University, Istanbul, Turkey
I.O. Atakisi, E. Gülmez, M. Kaya[63], O. Kaya[64], Ö. Özçelik, S. Tekten, E.A. Yetkin[65]

Istanbul Technical University, Istanbul, Turkey
A. Cakir, K. Cankocak, Y. Komurcu, S. Sen[66]

Istanbul University, Istanbul, Turkey
B. Kaynak, S. Ozkorucuklu

Institute for Scintillation Materials of National Academy of Science of Ukraine, Kharkov, Ukraine
B. Grynyov

National Scientific Center, Kharkov Institute of Physics and Technology, Kharkov, Ukraine
L. Levchuk

University of Bristol, Bristol, United Kingdom
E. Bhal, S. Bologna, J.J. Brooke, D. Burns[67], E. Clement, D. Cussans, H. Flacher, J. Goldstein, G.P. Heath, H.F. Heath, L. Kreczko, B. Krikler, S. Paramesvaran, B. Penning, T. Sakuma, S. Seif El Nasr-Storey, V.J. Smith, J. Taylor, A. Titterton

Rutherford Appleton Laboratory, Didcot, United Kingdom
K.W. Bell, A. Belyaev[68], C. Brew, R.M. Brown, D.J.A. Cockerill, J.A. Coughlan, K. Harder, S. Harper, J. Linacre, K. Manolopoulos, D.M. Newbold, E. Olaiya, D. Petyt, T. Reis, T. Schuh, C.H. Shepherd-Themistocleous, A. Thea, I.R. Tomalin, T. Williams, W.J. Womersley

Imperial College, London, United Kingdom
R. Bainbridge, P. Bloch, J. Borg, S. Breeze, O. Buchmuller, A. Bundock, GurpreetSingh CHAHAL[69], D. Colling, P. Dauncey, G. Davies, M. Della Negra, R. Di Maria, P. Everaerts, G. Hall, G. Iles, M. Komm, L. Lyons, A.-M. Magnan, S. Malik, A. Martelli, V. Milosevic, A. Morton, J. Nash[70], V. Palladino, M. Pesaresi, D.M. Raymond, A. Richards, A. Rose, E. Scott, C. Seez, A. Shtipliyski, M. Stoye, T. Strebler, A. Tapper, K. Uchida, T. Virdee[17], N. Wardle, D. Winterbottom, A.G. Zecchinelli, S.C. Zenz

Brunel University, Uxbridge, United Kingdom
J.E. Cole, P.R. Hobson, A. Khan, P. Kyberd, C.K. Mackay, I.D. Reid, L. Teodorescu, S. Zahid

Baylor University, Waco, USA
K. Call, B. Caraway, J. Dittmann, K. Hatakeyama, C. Madrid, B. McMaster, N. Pastika, C. Smith

Catholic University of America, Washington, DC, USA
R. Bartek, A. Dominguez, R. Uniyal, A.M. Vargas Hernandez

The University of Alabama, Tuscaloosa, USA
A. Buccilli, S.I. Cooper, C. Henderson, P. Rumerio, C. West

Boston University, Boston, USA
A. Albert, D. Arcaro, Z. Demiragli, D. Gastler, C. Richardson, J. Rohlf, D. Sperka, I. Suarez, L. Sulak, D. Zou

Brown University, Providence, USA
G. Benelli, B. Burkle, X. Coubez[18], D. Cutts, Y.t. Duh, M. Hadley, U. Heintz, J.M. Hogan[71], K.H.M. Kwok, E. Laird, G. Landsberg, K.T. Lau, J. Lee, M. Narain, S. Sagir[72], R. Syarif, E. Usai, W.Y. Wong, D. Yu, W. Zhang

University of California, Davis, Davis, USA
R. Band, C. Brainerd, R. Breedon, M. Calderon De La Barca Sanchez, M. Chertok, J. Conway, R. Conway, P.T. Cox, R. Erbacher, C. Flores, G. Funk, F. Jensen, W. Ko[†], O. Kukral, R. Lander, M. Mulhearn, D. Pellett, J. Pilot, M. Shi, D. Taylor, K. Tos, M. Tripathi, Z. Wang, F. Zhang

University of California, Los Angeles, USA
M. Bachtis, C. Bravo, R. Cousins, A. Dasgupta, A. Florent, J. Hauser, M. Ignatenko, N. Mccoll, W.A. Nash, S. Regnard, D. Saltzberg, C. Schnaible, B. Stone, V. Valuev

University of California, Riverside, Riverside, USA
K. Burt, Y. Chen, R. Clare, J.W. Gary, S.M.A. Ghiasi Shirazi, G. Hanson, G. Karapostoli, O.R. Long, M. Olmedo Negrete, M.I. Paneva, W. Si, L. Wang, S. Wimpenny, B.R. Yates, Y. Zhang

University of California, San Diego, La Jolla, USA
J.G. Branson, P. Chang, S. Cittolin, S. Cooperstein, N. Deelen, M. Derdzinski, R. Gerosa, D. Gilbert, B. Hashemi, D. Klein, V. Krutelyov, J. Letts, M. Masciovecchio, S. May, S. Padhi, M. Pieri, V. Sharma, M. Tadel, F. Würthwein, A. Yagil, G. Zevi Della Porta

University of California, Santa Barbara - Department of Physics, Santa Barbara, USA
N. Amin, R. Bhandari, C. Campagnari, M. Citron, V. Dutta, M. Franco Sevilla, J. Incandela, B. Marsh, H. Mei, A. Ovcharova, H. Qu, J. Richman, U. Sarica, D. Stuart, S. Wang

California Institute of Technology, Pasadena, USA
D. Anderson, A. Bornheim, O. Cerri, I. Dutta, J.M. Lawhorn, N. Lu, J. Mao, H.B. Newman, T.Q. Nguyen, J. Pata, M. Spiropulu, J.R. Vlimant, S. Xie, Z. Zhang, R.Y. Zhu

Carnegie Mellon University, Pittsburgh, USA
M.B. Andrews, T. Ferguson, T. Mudholkar, M. Paulini, M. Sun, I. Vorobiev, M. Weinberg

University of Colorado Boulder, Boulder, USA
J.P. Cumalat, W.T. Ford, E. MacDonald, T. Mulholland, R. Patel, A. Perloff, K. Stenson, K.A. Ulmer, S.R. Wagner

Cornell University, Ithaca, USA
J. Alexander, Y. Cheng, J. Chu, A. Datta, A. Frankenthal, K. Mcdermott, J.R. Patterson, D. Quach, A. Ryd, S.M. Tan, Z. Tao, J. Thom, P. Wittich, M. Zientek

Fermi National Accelerator Laboratory, Batavia, USA
S. Abdullin, M. Albrow, M. Alyari, G. Apollinari, A. Apresyan, A. Apyan, S. Banerjee, L.A.T. Bauerdick, A. Beretvas, D. Berry, J. Berryhill, P.C. Bhat, K. Burkett, J.N. Butler, A. Canepa, G.B. Cerati, H.W.K. Cheung, F. Chlebana, M. Cremonesi, J. Duarte, V.D. Elvira, J. Freeman, Z. Gecse, E. Gottschalk, L. Gray, D. Green, S. Grünendahl, O. Gutsche, AllisonReinsvold Hall, J. Hanlon, R.M. Harris, S. Hasegawa, R. Heller, J. Hirschauer, B. Jayatilaka, S. Jindariani, M. Johnson, U. Joshi, T. Klijnsma, B. Klima, M.J. Kortelainen, B. Kreis, S. Lammel, J. Lewis, D. Lincoln, R. Lipton, M. Liu, T. Liu, J. Lykken, K. Maeshima, J.M. Marraffino, D. Mason, P. McBride, P. Merkel, S. Mrenna, S. Nahn, V. O'Dell, V. Papadimitriou, K. Pedro, C. Pena, G. Rakness, F. Ravera, L. Ristori, B. Schneider, E. Sexton-Kennedy, N. Smith, A. Soha, W.J. Spalding, L. Spiegel, S. Stoynev, J. Strait, N. Strobbe, L. Taylor, S. Tkaczyk, N.V. Tran, L. Uplegger, E.W. Vaandering, C. Vernieri, R. Vidal, M. Wang, H.A. Weber

University of Florida, Gainesville, USA
D. Acosta, P. Avery, D. Bourilkov, A. Brinkerhoff, L. Cadamuro, V. Cherepanov, F. Errico, R.D. Field, S.V. Gleyzer, D. Guerrero, B.M. Joshi, M. Kim, J. Konigsberg, A. Korytov, K.H. Lo, K. Matchev, N. Menendez, G. Mitselmakher, D. Rosenzweig, K. Shi, J. Wang, S. Wang, X. Zuo

Florida International University, Miami, USA
Y.R. Joshi

Florida State University, Tallahassee, USA
T. Adams, A. Askew, S. Hagopian, V. Hagopian, K.F. Johnson, R. Khurana, T. Kolberg, G. Martinez, T. Perry, H. Prosper, C. Schiber, R. Yohay, J. Zhang

Florida Institute of Technology, Melbourne, USA
M.M. Baarmand, M. Hohlmann, D. Noonan, M. Rahmani, M. Saunders, F. Yumiceva

University of Illinois at Chicago (UIC), Chicago, USA
M.R. Adams, L. Apanasevich, R.R. Betts, R. Cavanaugh, X. Chen, S. Dittmer, O. Evdokimov, C.E. Gerber, D.A. Hangal, D.J. Hofman, C. Mills, T. Roy, M.B. Tonjes, N. Varelas, J. Viinikainen, H. Wang, X. Wang, Z. Wu

The University of Iowa, Iowa City, USA
M. Alhusseini, B. Bilki[56], K. Dilsiz[73], S. Durgut, R.P. Gandrajula, M. Haytmyradov, V. Khristenko, O.K. Köseyan, J.-P. Merlo, A. Mestvirishvili[74], A. Moeller, J. Nachtman, H. Ogul[75], Y. Onel, F. Ozok[76], A. Penzo, C. Snyder, E. Tiras, J. Wetzel

Johns Hopkins University, Baltimore, USA
B. Blumenfeld, A. Cocoros, N. Eminizer, A.V. Gritsan, W.T. Hung, S. Kyriacou, P. Maksimovic, J. Roskes, M. Swartz

The University of Kansas, Lawrence, USA
C. Baldenegro Barrera, P. Baringer, A. Bean, S. Boren, J. Bowen, A. Bylinkin, T. Isidori, S. Khalil, J. King, G. Krintiras, A. Kropivnitskaya, C. Lindsey, D. Majumder, W. Mcbrayer, N. Minafra, M. Murray, C. Rogan, C. Royon, S. Sanders, E. Schmitz, J.D. Tapia Takaki, Q. Wang, J. Williams, G. Wilson

Kansas State University, Manhattan, USA
S. Duric, A. Ivanov, K. Kaadze, D. Kim, Y. Maravin, D.R. Mendis, T. Mitchell, A. Modak, A. Mohammadi

Lawrence Livermore National Laboratory, Livermore, USA
F. Rebassoo, D. Wright

University of Maryland, College Park, USA
A. Baden, O. Baron, A. Belloni, S.C. Eno, Y. Feng, N.J. Hadley, S. Jabeen, G.Y. Jeng, R.G. Kellogg, A.C. Mignerey, S. Nabili, F. Ricci-Tam, M. Seidel, Y.H. Shin, A. Skuja, S.C. Tonwar, K. Wong

Massachusetts Institute of Technology, Cambridge, USA
D. Abercrombie, B. Allen, A. Baty, R. Bi, S. Brandt, W. Busza, I.A. Cali, M. D'Alfonso, G. Gomez Ceballos, M. Goncharov, P. Harris, D. Hsu, M. Hu, M. Klute, D. Kovalskyi, Y.-J. Lee, P.D. Luckey, B. Maier, A.C. Marini, C. Mcginn, C. Mironov, S. Narayanan, X. Niu, C. Paus, D. Rankin, C. Roland, G. Roland, Z. Shi, G.S.F. Stephans, K. Sumorok, K. Tatar, D. Velicanu, J. Wang, T.W. Wang, B. Wyslouch

University of Minnesota, Minneapolis, USA
R.M. Chatterjee, A. Evans, S. Guts†, P. Hansen, J. Hiltbrand, Sh. Jain, Y. Kubota, Z. Lesko, J. Mans, M. Revering, R. Rusack, R. Saradhy, N. Schroeder, M.A. Wadud

University of Mississippi, Oxford, USA
J.G. Acosta, S. Oliveros

University of Nebraska-Lincoln, Lincoln, USA
K. Bloom, S. Chauhan, D.R. Claes, C. Fangmeier, L. Finco, F. Golf, R. Kamalieddin, I. Kravchenko, J.E. Siado, G.R. Snow†, B. Stieger, W. Tabb

State University of New York at Buffalo, Buffalo, USA
G. Agarwal, C. Harrington, I. Iashvili, A. Kharchilava, C. McLean, D. Nguyen, A. Parker, J. Pekkanen, S. Rappoccio, B. Roozbahani

Northeastern University, Boston, USA
G. Alverson, E. Barberis, C. Freer, Y. Haddad, A. Hortiangtham, G. Madigan, B. Marzocchi, D.M. Morse, T. Orimoto, L. Skinnari, A. Tishelman-Charny, T. Wamorkar, B. Wang, A. Wisecarver, D. Wood

Northwestern University, Evanston, USA
S. Bhattacharya, J. Bueghly, A. Gilbert, T. Gunter, K.A. Hahn, N. Odell, M.H. Schmitt, K. Sung, M. Trovato, M. Velasco

University of Notre Dame, Notre Dame, USA
R. Bucci, N. Dev, R. Goldouzian, M. Hildreth, K. Hurtado Anampa, C. Jessop, D.J. Karmgard, K. Lannon, W. Li, N. Loukas, N. Marinelli, I. Mcalister, F. Meng, Y. Musienko[38], R. Ruchti, P. Siddireddy, G. Smith, S. Taroni, M. Wayne, A. Wightman, M. Wolf, A. Woodard

The Ohio State University, Columbus, USA
J. Alimena, B. Bylsma, L.S. Durkin, B. Francis, C. Hill, W. Ji, A. Lefeld, T.Y. Ling, B.L. Winer

Princeton University, Princeton, USA
G. Dezoort, P. Elmer, J. Hardenbrook, N. Haubrich, S. Higginbotham, A. Kalogeropoulos, S. Kwan, D. Lange, M.T. Lucchini, J. Luo, D. Marlow, K. Mei, I. Ojalvo, J. Olsen, C. Palmer, P. Piroué, D. Stickland, C. Tully

University of Puerto Rico, Mayaguez, USA
S. Malik, S. Norberg

Purdue University, West Lafayette, USA
A. Barker, V.E. Barnes, S. Das, L. Gutay, M. Jones, A.W. Jung, A. Khatiwada, B. Mahakud, D.H. Miller, G. Negro, N. Neumeister, C.C. Peng, S. Piperov, H. Qiu, J.F. Schulte, N. Trevisani, F. Wang, R. Xiao, W. Xie

Purdue University Northwest, Hammond, USA
T. Cheng, J. Dolen, N. Parashar

Rice University, Houston, USA
U. Behrens, K.M. Ecklund, S. Freed, F.J.M. Geurts, M. Kilpatrick, Arun Kumar, W. Li, B.P. Padley, R. Redjimi, J. Roberts, J. Rorie, W. Shi, A.G. Stahl Leiton, Z. Tu, A. Zhang

University of Rochester, Rochester, USA
A. Bodek, P. de Barbaro, R. Demina, J.L. Dulemba, C. Fallon, T. Ferbel, M. Galanti, A. Garcia-Bellido, O. Hindrichs, A. Khukhunaishvili, E. Ranken, R. Taus

Rutgers, The State University of New Jersey, Piscataway, USA
B. Chiarito, J.P. Chou, A. Gandrakota, Y. Gershtein, E. Halkiadakis, A. Hart, M. Heindl, E. Hughes, I. Laflotte, A. Lath, R. Montalvo, K. Nash, M. Osherson, H. Saka, S. Salur, S. Schnetzer, S. Somalwar, R. Stone, S. Thomas, J. Vora

University of Tennessee, Knoxville, USA
H. Acharya, A.G. Delannoy, S. Spanier

Texas A&M University, College Station, USA
O. Bouhali[77], M. Dalchenko, M. De Mattia, A. Delgado, S. Dildick, R. Eusebi, J. Gilmore, T. Huang, T. Kamon[78], H. Kim, S. Luo, S. Malhotra, D. Marley, R. Mueller, D. Overton, L. Perniè, D. Rathjens, A. Safonov

Texas Tech University, Lubbock, USA
N. Akchurin, J. Damgov, F. De Guio, V. Hegde, S. Kunori, K. Lamichhane, S.W. Lee, T. Mengke, S. Muthumuni, T. Peltola, S. Undleeb, I. Volobouev, Z. Wang, A. Whitbeck

Vanderbilt University, Nashville, USA
S. Greene, A. Gurrola, R. Janjam, W. Johns, C. Maguire, A. Melo, H. Ni, K. Padeken, F. Romeo, P. Sheldon, S. Tuo, J. Velkovska, M. Verweij

University of Virginia, Charlottesville, USA
M.W. Arenton, P. Barria, B. Cox, G. Cummings, J. Hakala, R. Hirosky, M. Joyce, A. Ledovskoy, C. Neu, B. Tannenwald, Y. Wang, E. Wolfe, F. Xia

Wayne State University, Detroit, USA
R. Harr, P.E. Karchin, N. Poudyal, J. Sturdy, P. Thapa

University of Wisconsin - Madison, Madison, WI, USA
T. Bose, J. Buchanan, C. Caillol, D. Carlsmith, S. Dasu, I. De Bruyn, L. Dodd, C. Galloni, H. He, M. Herndon, A. Hervé, U. Hussain, A. Lanaro, A. Loeliger, K. Long, R. Loveless, J. Madhusudanan Sreekala, D. Pinna, T. Ruggles, A. Savin, V. Sharma, W.H. Smith, D. Teague, S. Trembath-reichert

†: Deceased
1: Also at Vienna University of Technology, Vienna, Austria
2: Also at IRFU, CEA, Université Paris-Saclay, Gif-sur-Yvette, France
3: Also at Universidade Estadual de Campinas, Campinas, Brazil
4: Also at Federal University of Rio Grande do Sul, Porto Alegre, Brazil
5: Also at UFMS, Nova Andradina, Brazil
6: Also at Universidade Federal de Pelotas, Pelotas, Brazil
7: Also at Université Libre de Bruxelles, Bruxelles, Belgium
8: Also at University of Chinese Academy of Sciences, Beijing, China
9: Also at Institute for Theoretical and Experimental Physics named by A.I. Alikhanov of NRC 'Kurchatov Institute', Moscow, Russia
10: Also at Joint Institute for Nuclear Research, Dubna, Russia
11: Also at Suez University, Suez, Egypt
12: Now at British University in Egypt, Cairo, Egypt
13: Also at Purdue University, West Lafayette, USA
14: Also at Université de Haute Alsace, Mulhouse, France
15: Also at Tbilisi State University, Tbilisi, Georgia
16: Also at Erzincan Binali Yildirim University, Erzincan, Turkey
17: Also at CERN, European Organization for Nuclear Research, Geneva, Switzerland

18: Also at RWTH Aachen University, III. Physikalisches Institut A, Aachen, Germany
19: Also at University of Hamburg, Hamburg, Germany
20: Also at Brandenburg University of Technology, Cottbus, Germany
21: Also at Institute of Physics, University of Debrecen, Debrecen, Hungary, Debrecen, Hungary
22: Also at Institute of Nuclear Research ATOMKI, Debrecen, Hungary
23: Also at MTA-ELTE Lendület CMS Particle and Nuclear Physics Group, Eötvös Loránd University, Budapest, Hungary, Budapest, Hungary
24: Also at IIT Bhubaneswar, Bhubaneswar, India, Bhubaneswar, India
25: Also at Institute of Physics, Bhubaneswar, India
26: Also at Shoolini University, Solan, India
27: Also at University of Hyderabad, Hyderabad, India
28: Also at University of Visva-Bharati, Santiniketan, India
29: Also at Isfahan University of Technology, Isfahan, Iran
30: Now at INFN Sezione di Bari [a], Università di Bari [b], Politecnico di Bari [c], Bari, Italy
31: Also at Italian National Agency for New Technologies, Energy and Sustainable Economic Development, Bologna, Italy
32: Also at Centro Siciliano di Fisica Nucleare e di Struttura Della Materia, Catania, Italy
33: Also at Scuola Normale e Sezione dell'INFN, Pisa, Italy
34: Also at Riga Technical University, Riga, Latvia, Riga, Latvia
35: Also at Malaysian Nuclear Agency, MOSTI, Kajang, Malaysia
36: Also at Consejo Nacional de Ciencia y Tecnología, Mexico City, Mexico
37: Also at Warsaw University of Technology, Institute of Electronic Systems, Warsaw, Poland
38: Also at Institute for Nuclear Research, Moscow, Russia
39: Now at National Research Nuclear University 'Moscow Engineering Physics Institute' (MEPhI), Moscow, Russia
40: Also at St. Petersburg State Polytechnical University, St. Petersburg, Russia
41: Also at University of Florida, Gainesville, USA
42: Also at Imperial College, London, United Kingdom
43: Also at P.N. Lebedev Physical Institute, Moscow, Russia
44: Also at California Institute of Technology, Pasadena, USA
45: Also at Budker Institute of Nuclear Physics, Novosibirsk, Russia
46: Also at Faculty of Physics, University of Belgrade, Belgrade, Serbia
47: Also at Università degli Studi di Siena, Siena, Italy
48: Also at INFN Sezione di Pavia [a], Università di Pavia [b], Pavia, Italy, Pavia, Italy
49: Also at National and Kapodistrian University of Athens, Athens, Greece
50: Also at Universität Zürich, Zurich, Switzerland
51: Also at Stefan Meyer Institute for Subatomic Physics, Vienna, Austria, Vienna, Austria
52: Also at Burdur Mehmet Akif Ersoy University, BURDUR, Turkey
53: Also at Adiyaman University, Adiyaman, Turkey
54: Also at Şırnak University, Sirnak, Turkey
55: Also at Tsinghua University, Beijing, China
56: Also at Beykent University, Istanbul, Turkey, Istanbul, Turkey
57: Also at Istanbul Aydin University, Istanbul, Turkey
58: Also at Mersin University, Mersin, Turkey
59: Also at Piri Reis University, Istanbul, Turkey
60: Also at Gaziosmanpasa University, Tokat, Turkey
61: Also at Ozyegin University, Istanbul, Turkey
62: Also at Izmir Institute of Technology, Izmir, Turkey

63: Also at Marmara University, Istanbul, Turkey
64: Also at Kafkas University, Kars, Turkey
65: Also at Istanbul Bilgi University, Istanbul, Turkey
66: Also at Hacettepe University, Ankara, Turkey
67: Also at Vrije Universiteit Brussel, Brussel, Belgium
68: Also at School of Physics and Astronomy, University of Southampton, Southampton, United Kingdom
69: Also at IPPP Durham University, Durham, United Kingdom
70: Also at Monash University, Faculty of Science, Clayton, Australia
71: Also at Bethel University, St. Paul, Minneapolis, USA, St. Paul, USA
72: Also at Karamanoğlu Mehmetbey University, Karaman, Turkey
73: Also at Bingol University, Bingol, Turkey
74: Also at Georgian Technical University, Tbilisi, Georgia
75: Also at Sinop University, Sinop, Turkey
76: Also at Mimar Sinan University, Istanbul, Istanbul, Turkey
77: Also at Texas A&M University at Qatar, Doha, Qatar
78: Also at Kyungpook National University, Daegu, Korea, Daegu, Korea